AD_____

AWARD NUMBER: W81XWH-06-1-0417

TITLE: Immunology, Systems Biology, and Immunotherapy of Breast Cancer

PRINCIPAL INVESTIGATOR: Peter P. Lee, M.D.

CONTRACTING ORGANIZATION: Stanford University
Stanford, CA 94305

REPORT DATE: March 2010

TYPE OF REPORT: Annual

PREPARED FOR: U.S. Army Medical Research and Materiel Command
Fort Detrick, Maryland 21702-5012

DISTRIBUTION STATEMENT: Approved for Public Release;
Distribution Unlimited

The views, opinions and/or findings contained in this report are those of the author(s) and should not be construed as an official Department of the Army position, policy or decision unless so designated by other documentation.

REPORT DOCUMENTATION PAGE

Form Approved
OMB No. 0704-0188

Public reporting burden for this collection of information is estimated to average 1 hour per response, including the time for reviewing instructions, searching existing data sources, gathering and maintaining the data needed, and completing and reviewing this collection of information. Send comments regarding this burden estimate or any other aspect of this collection of information, including suggestions for reducing this burden to Department of Defense, Washington Headquarters Services, Directorate for Information Operations and Reports (0704-0188), 1215 Jefferson Davis Highway, Suite 1204, Arlington, VA 22202-4302. Respondents should be aware that notwithstanding any other provision of law, no person shall be subject to any penalty for failing to comply with a collection of information if it does not display a currently valid OMB control number. **PLEASE DO NOT RETURN YOUR FORM TO THE ABOVE ADDRESS.**

1. REPORT DATE	2. REPORT TYPE	3. DATES COVERED
1 March 2010	Annual	1 Mar 2009 – 28 Feb 2010

4. TITLE AND SUBTITLE

Immunology, Systems Biology, and Immunotherapy of Breast Cancer

5a. CONTRACT NUMBER

5b. GRANT NUMBER
W81XWH-06-1-0417

5c. PROGRAM ELEMENT NUMBER

6. AUTHOR(S)

Peter P. Lee, M.D.

E-Mail: ppl@stanford.edu

5d. PROJECT NUMBER

5e. TASK NUMBER

5f. WORK UNIT NUMBER

7. PERFORMING ORGANIZATION NAME(S) AND ADDRESS(ES)

Stanford University
Stanford, CA 94305

8. PERFORMING ORGANIZATION REPORT NUMBER

9. SPONSORING / MONITORING AGENCY NAME(S) AND ADDRESS(ES)
U.S. Army Medical Research and Materiel Command
Fort Detrick, Maryland 21702-5012

10. SPONSOR/MONITOR'S ACRONYM(S)

11. SPONSOR/MONITOR'S REPORT NUMBER(S)

12. DISTRIBUTION / AVAILABILITY STATEMENT
Approved for Public Release; Distribution Unlimited

13. SUPPLEMENTARY NOTES

14. ABSTRACT
In year 4, the foundation we have built over the first three years of this award have enabled us to make substantial progress in multiple areas of this project. We now have an efficient system in place to recruit patients into this study and procure their samples, with a total of 240 subjects recruited to-date. Limited amounts of clinical materials available from each subject remains major challenges to the success of this project – we continually attempt to address and solve this issue by reducing the cell numbers that we need for each assay. We have further enhanced and refined a powerful set of immunological assays and molecular tools to study these samples in greater detail than previously possible. We continue to uncover dramatic changes in the immune cell populations within tumors, TDLNs, and peripheral blood from breast cancer patients. These findings are reported above, and have led to a high profile publication in PNAS, with more to come in year 5. The coming final year of this award will see more progress and insights.

15. SUBJECT TERMS
Breast cancer, immunology, immunotherapy, systems biology

16. SECURITY CLASSIFICATION OF:			17. LIMITATION OF ABSTRACT	18. NUMBER OF PAGES	19a. NAME OF RESPONSIBLE PERSON
a. REPORT	b. ABSTRACT	c. THIS PAGE			USAMRMC
U	U	U	UU	41	19b. TELEPHONE NUMBER *(include area code)*

Table of Contents

Annual Progress Report 3/1/09-2/28/10
DoD Era of Hope Scholar Award
Immunology, Systems Biology, and Immunotherapy of Breast Cancer
Peter P. Lee, M.D.
Stanford University

INTRODUCTION

Breast cancer patients with similar tumor characteristics may have vastly different clinical courses, response to therapy, and outcome. Several lines of evidence now suggest that the host immune response may play a significant role in modulating disease progression in cancer. A complex interplay exists between the host immune response and tumor cells as a critical determinant in clinical outcome. These factors remain poorly understood. By comprehensively studying the dynamics between breast cancer and the immune response using an integrative systems approach, we hope to uncover opportunities for vastly different immunotherapy approaches than what are available today. We seek to move beyond the current paradigm of eliciting immune responses against defined antigens via vaccination, as this strategy alone does not appear to be effective in a number of clinical trials for melanoma and other cancers. Rather, we seek strategies that specifically modulate tumor-immune cell interactions and block cancer-induced immune dysfunction on a systemic and local level (at tumor sites and draining lymph nodes). In this project, we use a number of novel immunological approaches to look for evidence of immune cell dysfunction within the tumor or tumor-draining lymph nodes (TDLNs) from breast cancer patients. This includes archived samples from patients with at least five year survival data, and fresh samples from newly diagnosed patients. We use DNA microarrays to analyze the gene expression patterns of purified tumor and immune cells, focusing on gene networks and cross-talk between tumor and immune cells. We generate high-resolution images of tumor and TDLN sections and develop image analysis algorithms to assess the spatial arrangement and grouping of tumor and immune cells with respect to each other that may have biological significance. Using statistics and mathematical tools, we will integrate the complex data generated from all of these studies and correlate them with clinical parameters. Lastly, our observations will be combined into a mathematical model that will enable us to perform *in silico* experiments to quickly test novel therapeutic strategies for breast cancer. This work may lead to novel diagnostic tools to help predict clinical outcome and guide therapy in breast cancer patients. We also hope to find new insights into the mechanisms of immune evasion by breast cancer cells and ultimately new treatment strategies for breast cancer directed specifically at altering the biology of TDLNs.

BODY

Our team currently consists of two excellent postdoctoral fellows, one research assistant, and several faculty collaborators (only one of which draws a modest amount of salary support from this award). We work closely with our surgery, medical oncology, and pathology colleagues to identify, recruit, and consent subjects, and to obtain samples from the operating room to pathology and eventually to my laboratory. In addition, we continue to refine our protocols to maximize recovery of immune cells from tumor and lymph node specimens, and to optimize methods for analysis of fresh and archive samples by flow cytometry, immunohistology, immunoflourescence, function assays, and DNA microarray analysis using the smallest numbers

of cells possible. Below is a summary of our progress in year 4 of our EHSA in relation to my proposed SOW.

Experiment Strategy

To fully understand tumor-immune cell interactions in breast cancer, our strategy is to compare the immune cells and tumor cells within three distinct compartments: the tumor, TDLNs, and blood. We approach this at both the molecular and cellular levels. At the molecular level, gene expression profiling of immune cells and tumor cells within the tumor site and TDLNs are being carried out. At the cellular level, immunologic functions of immune cells are being studied and compared across these three compartments.

A. Immunological Analyses

Originally proposed in the SOW:
1. Analysis of archived samples of tumor and TDLN from breast cancer patients with at least 5 years of clinical follow-up data. Tumor and immune cell markers will be identified via immunohistochemical (IHC) staining and in-situ hybridization (ISH). Images will be acquired in high resolution using an automated imaging system (BLISS), and data will be acquired using automated software. Over 50 immune and tumor markers will be assessed. To facilitate these complex studies, we will also explore the use of tissue microarrays (TMA). This would enable us to analyze sections from 100-400 samples on each slide. We will first perform a pilot study to ensure that the TMA method is compatible for our studies and would not be negatively impacted by the architectural heterogeneity within TDLN. (months 0-60)
2. Analysis of live cells from fresh tumor, TDLN, blood, and possibly bone marrow from newly diagnosed or relapsed breast cancer patients undergoing surgery or treatment. Assays include flow cytometry (up to 12 colors), peptide-MHC tetramer analysis, sorting, functional responses (e.g. cytotoxicity, cytokine release, anergy, apoptosis, proliferation), and others. (months 6-60)
3. Generation of T cell lines and tumor cell lines from fresh tumor and TDLN samples for further detailed analyses. (months 6-60)
4. If the above studies demonstrate immune cell dysfunction within tumor or TDLN, but by themselves do not reveal any definitive mechanisms, then we will undertake in vivo studies with mouse models of de novo breast cancer to address the early events in immune dysfunction. (months 24-60)

Sample Acquisition
At the end of year 4, over 240 breast cancer patients have been enrolled into this study. All participants were newly diagnosed, had recurrent or metastatic disease and had their surgical and/or oncological treatments at Stanford University Medical Center. Written informed consents were obtained from all participants according to Stanford IRB, DoD HSRRB, and HIPAA regulations. Patients' heparinized peripheral blood samples, breast tumor tissue, TDLNs (non-sentinel lymph node and/or sentinel lymph node), and tumor/TDLN aspirates have been collected for this study. Clinical data (stage, grade, ER/PR/Her-2/neu status, treatment, and clinical outcome) for each participant has been recorded.

Interferon Signaling Defect in Lymphocytes from Breast Cancer, Melanoma, and Gastrointestinal Patients

Previously we demonstrated Interferon (IFN) signaling defects in lymphocytes from patients with melanoma, as measured by microarray, Q-PCR, and Phosflow analysis (Critchley-Thorne, R., *et al,* 2007). Recently, we further demonstrated that this phenomenon also occurs in lymphocytes from patients with breast cancer, which exhibit reduced IFN signaling pathway activity as compared with lymphocytes from age-matched healthy controls as measured by Q-PCR, Phosflow analysis, and functional analyses (Critchley-Thorne, R., *et al,* 2009). Lymphocytes from breast cancer patients had downregulated basal expression levels of IFN-stimulated genes (ISGs), significantly reduced fold induction of STAT1-Y701 phosphorylation (pSTAT1) in response to IFN-α stimulation in CD3+ T cells, CD19+ B cells, CD16+ Natural Killer (NK) cells, and CD4+CD45RO+CD25 ^{HI} regulatory T cells (Treg), and significantly reduced fold induction of pSTAT1 in response to IFN-γ in CD19+ B cells, regardless of neoadjuvant/adjuvant therapy. Furthermore, defective pSTAT1 activation in response to IFN-α and IFN-γ was observed in breast cancer stages II, III and IV illustrating this immune defect occurs in early stage breast cancer.

Mechanistic Study for Type I and Type II IFN Pathway Defects in Cancer

- Expression of IFN Receptors
- Expression of Signaling Regulators
- Phosflow Analysis of pSTATs Interrogatated by IFNs and Other Cytokines to Address Crosstalk between the IFN Pathway and Other Cytokine Pathways

To determine the mechanisms conferring defective IFN responses, we are examining the hypothesis that altered expression of IFN receptors or IFN signaling pathway regulators may contribute to IFN hypo-responsiveness in cancer patients. As an alternate hypothesis we are addressing whether altered cross-talk with other cytokine signaling pathways contributes to defective IFN-pSTAT1 signaling by analyzing pSTATs in response to IFNs and other cytokines which cross-talk with the IFN pathway. In addition, we will extend our previous studies by determining if IFN defects occur in myeloid lineage immune cells and if IFN defects occur as early as stage 0 in breast cancer patients. We will also examine whether signaling pathways that lead to production of IFNs are intact in cancer patient PBMCs. IFN-γ is induced primarily in response to IL-12-STAT4 signaling in NK and T cells. IFN-α/β are induced in response to members of toll-like receptor (TLR) family and the RIG-I like receptor (RLR) family signaling pathways through TBK1 and NF-κB. Thus, TBK1 and NF-κB activation in response to the TLR4 ligand LPS and the dsDNA ligand polydA-dT:dT-dA will be determined. In this latest study, we will analyze PBMCs from a new cohort of 34 breast cancer and 22 age-matched healthy controls (Table A1).

Table A1: Patient Characteristics

GROUP	**AGE**			**STAGE**					**Male**	**Female**	**TOTAL**
	Mean	**Median**	**Range**	**0**	**1**	**2**	**3**	**4**	**N=**	**N=**	**N=**
Healthy	49.182	51	18-82						6	16	22
Breast Cancer	54.105	53	31-85	7	7	8	7	5	0	34	34

Analysis of IFN receptor expression on PBMCs from breast cancer patients

Cryopreserved PBMCs from this new patient cohort (Table A1) were thawed and rested overnight before staining for immune cell surface markers, IFN-αR1, IFN-αR2, and IFN-γR1, and analyzed on a LSRII flow cytometer. Cells were classified as monocytes (CD33+), B cells (CD19+), NK cells (CD16+), and T cells (CD4+ or CD8+). Within the CD4+ or CD8+ populations, cells were defined as naïve (CD45RA+) or memory (CD45RA-). Data was normalized to an internal control and analyzed using two-sided Wilcoxon-Mann-Whitney test (95% CI) to calculate p-values for each of the comparisons. P-values of < 0.05 will be considered significant.

In preliminary analysis, several interesting observations have been noted. Median IFN-αR1 expression was similar in all healthy versus breast cancer immune cell subtypes except for memory CD8 T cells (CD8+CD45RA-), in which breast cancer patients had significantly elevated levels of IFN-αR1 expression (Figure A1). Median IFN-αR2 expression levels were similar in all healthy versus breast cancer immune cell subtypes (Figure A2). Median IFN-γR1 expression was significantly lower in breast cancer patient immune populations including CD4+ T cells, particularly naïve CD4+ T cells (CD4+CD45RA+), memory CD8+ T cells (CD8+CD45RA-), and NK cells (CD16+) compared with healthy controls (Figure A3). Thus, differences in expression levels of IFN receptors, particularly IFN-γR1, may play a role in IFN signaling defects observed in breast cancer patients, and this possibility will be explored further by correlating these IFN receptor expressions with p-STAT1 levels in response to IFN-α and IFN-γ stimulation.

Analysis of expression of IFN signaling pathway regulators in PBMCs from cancer patients

Cryopreserved PBMCs from this new patient cohort were thawed (Table A1) and rested overnight before total PBMC populations were preserved in Trizol at -80C. RNA will be isolated, quantified, and cDNA synthesized for Q-PCR analysis of expression of known IFN signaling pathway regulators.

Phosflow analysis of STAT phosphoryation in response to IFNs and other cytokines

Cryopreserved PBMCs from this new patient cohort (Table A1) were thawed and rested overnight before stimulation with cytokines or left unstimulated for 15 minutes (Table A2). The samples were then fixed and permeabilized in methanol and stored at -80C to await antibody staining and flow cytometry analysis. Tyrosine phosphorylation of specific STAT family members will be analyzed for each stimulus and compared with corresponding unstimulated controls (Table A2).

Table A2:

	Stimulus	Stimulus concentration	pSTATs	Primary Cell Types Activated
1	IFN-α	1000 U/ml	pSTAT1, pSTAT3	All
2	IFN-γ	100 U/ml	pSTAT1, pSTAT3	B cells, Monocytes
3	IL-10	100ng/ml	pSTAT1, pSTAT3	All
4	IL-6	100 ng/ml	pSTAT1, pSTAT3	T cells
5	IL-27	50ng/ml	pSTAT1, pSTAT3	T & B cells
6	IL-2	100 ng/ml	pSTAT3, pSTAT5	T & NK cells
7	IL-7	1 ng/ml	pSTAT3, pSTAT5	T cells
8	GM-CSF	10ng/ml	pSTAT3, pSTAT5	Monocytes
9	IL-4	100 ng/ml	pSTAT6	T & B cells, Monocytes
10	IL-12	100 ng/ml	pSTAT4	T & NK cells

Phosflow analysis of TLR and RLR pathways in PBMCs from cancer patients

Cryopreserved PBMCs from this new patient cohort (Table A1) were thawed and rested overnight before stimulation with 10ng/ml LPS, transfection with 10ug/ml polydA-dT:dT-dA (complexed with Lipofectamine 2000) or left unstimulated for 15 minutes. The samples were then fixed and permeabilized in methanol and stored at -80C to await antibody staining and flow cytometry analysis. Phosphorylation of TBK1 and NF-κB will be analyzed for each stimulus and compared with corresponding unstimulated controls.

Cancer patient groups and healthy controls are composed of different ratios of males and females (Table A1), so we will first determine whether samples from different genders statistically differ from each other before within each group for each parameter analyzed before selecting appropriate healthy control groups. We have previously shown that IFN-α and IFN-γ activated STAT1-pY701was not statistically different between male and females among healthy controls, or within the melanoma and GI groups (Critchley-Thorne, R., *et al*, 2009). In addition, the mean ages differ for each cancer type, and thus the affect of age on each parameter will be analyzed before selecting appropriate healthy control groups for comparisons (Table A1).

Comprehensive IFN signaling pathway analysis by Luminex.

We previously attempted to optimize protocols to use a new system, Firefly 3000 (Cell Biosciences) to detect total STAT1 and STAT1-pY701. However, the results from this system were not optimal and we have since determined to use a more high-throughput multiplex Luminex system to comprehensively analyze IFN signaling pathways in cancer patient immune cells. Blood will be processed by Ficoll gradient to isolate PBMCs. Monocyte and lymphocyte populations will be separated using magnetic beads targeting CD14 expressed on monocytes. Monocytes will be stimulated with IFN-α, IFN-γ, IL-10, and LPS. Lymphocytes will be stimulated with IFN-α, IFN-γ, IL-10, IL-6, IL-27, and LPS. LPS will be used as a control for strong activation of MAPK and NF-κB pathways. Cell lysates will be incubated with a cocktail of commercially available Luminex beads conjugated to antibodies recognizing the phosphorylated forms of STATs, upstream JAK/TYK kinases, and the coordinately activated

MAPK and NF-κB pathways, and analyzed on the Luminex 200 machine. Total GAPDH will be measured as a loading control.

Generalization from Local to Systemic Tolerance

We believe that tumor-induced local tolerance in tumor-draining lymph nodes (TDLNs) is continually exerting effects on systemic tolerance to tumor associated antigens (TAAs). The TDLNs might progressively induce effector immune cell anergy as the cells transit through the TDLNs. Although it seems unlikely that a single lymph node could lead to the whole immune system tolerance, it has been reported previously that a mucosal-draining LN is capable of generating systemic tolerance (Kraal, *et al*., 2006). Therefore, we decided to functionally interrogate peripheral blood T cell and B cell responses through the crosslinking of the T cell receptor (TCR) and B cell receptor (BCR), respectively.

Phosflow Analysis on TCR signaling

PBMCs from 6 breast cancer and 7 age-matched healthy controls were stimulated with anti-CD3 (10ug/ml) and/or anti-CD28 (10ug/ml) or left unstimulated for 5 minutes. The cells were then fixed and permeabilized for Phosflow analysis using LSRII. The samples were stained with antibodies to CD20 (B cells), CD3, CD4, CD45RA as well as pZAP70, pSLP76 to determine the integrity of TCR signaling upon TCR crosslinking.

Preliminary results showed a skewed memory T cell phenotype over naïve T cell proportion**.** The proportion of memory T cells (CD45RA-) over naïve T cells (CD45RA+) is significantly higher in patients compared to healthy controls (Figure A4a). Lymphopenia is often seen in late stage cancer patients and aged populations. This might be due to increased apoptosis of naïve T cells and homeostatic proliferation memory T cells in the blood pool. Correlation with patient stages and age will be performed in a larger dataset to clarify this.

Preliminary results also showed the anti-CD3 induced phosphorylation of both SLP76 and ZAP70 in patient naïve CD4 T cells to be reduced in breast cancer patients compared to healthy controls. Anti-CD3 stimulation and costimulation with anti-CD28 did not rescue the reduced pSLP76 and pZAP70 level (Figure A4b). In contrast, this is not observed in memory CD4 T cells or CD8 T cells. Decreased TCR signaling could lead to shorter lifespan of naïve CD4 T cells. Naïve T cells, especially naïve CD4 T cells, constantly circulate through secondary lymphoid organs for homeostatic proliferation. Immune suppressed TDLNs might have induced anergic naïve CD4 T cells and progressively lead to systemic tolerance. A total of 30 breast cancer patients and 20 age-matched healthy controls' PBMCs will be assayed for TCR signaling phosflow analysis to confirm the current findings.

Altered circulating B cell Phenotype and BCR signaling in Breast Cancer Patients

PBMCs from 30 breast cancer and 20 age-matched healthy controls were stimulated with anti-IgM (2ug/ml) and anti-IgG (2ug/ml) or left unstimulated for 2 minutes. The cells were then fixed and permeabilized for Phosflow analysis using LSRII. The samples were stained with antibodies to CD20, CD3, CD27 (memory B cell marker) as well as pPLCγ2 and pERK1/2 to determine the integrity of BCR signaling upon BCR crosslinking.

The proportion of memory B cells (CD27+) over naïve B cells (CD27-) in breast cancer patients is significantly lower compared to healthy controls (Figure A5a). This is consistent with a recent publication suggesting that collapse of CD27 memory B cell compartment is a common phenomenon in cancer patients (Carpenter, *et al*, 2009). The surface expressions of IgG and IgM were also analyzed by FACS to determine the receptor level for anti-IgM and anti-IgG stimulations in patients and controls. Above 95% of CD27- B cells express surface IgM in both breast cancer patients and healthy controls, indicating that the majority of these cells have not gone through antibody isotype switch and, therefore, display a naïve phenotype. The percentage of IgM and/or IgG B cells varies from 10% to 90% in the memory B cell population; however, the distribution of IgM+ and/or IgG+ memory B cells showed no difference between breast cancer patients and healthy controls (Figure A5b).

Fold induction of pPLCγ2 and pERK1/2 in memory B cells (CD27+) was significantly reduced in patients compared to healthy controls in response to anti-IgM/anti-IgG stimulation. In contrast, the fold induction of pPLCγ2 and pERK1/2 in naive B cells (CD27-) was similar in breast cancer patients versus healthy controls (Figure A5c-d). The reduced phosphorylation of PLCγ2 and ERK1/2 in memory B cells did not correlate with the distribution of IgM+ and/or IgG+ memory B cells in breast cancer patients and controls. Naïve B cells encounter antigen, go through somatic hypermutation, isotype switch and affinity maturation in secondary lymphoid organs. We hypothesize that B cell dysfunctions in the circulations are due to blunted B cell differentiation and maturation in TDLNs. Dysfunctional B cells are being released from tolerized TDLNs and this might explain the suboptimal level of antibody against tumor-associated antigen in cancer patients. However, it is currently unknown whether this B cell dysfunction will influence the total antibody level in cancer patients. Antibody isotyping using Luminex will be used to assess the serum antibody level in breast cancer patients.

Summary of major findings and plans:

<u>IFN signaling perturbations in breast cancer leukocytes</u>

- We have demonstrated a defect in IFN signaling in peripheral blood lymphocytes from patients with breast cancer. Furthermore, we have shown that these defects are widespread as defects in IFN responses occurred in breast cancer patients, regardless of therapy, and regardless of naive, effector, or memory status.
- To determine the extent of the IFN defect, we will continue to use phosflow to examine pSTAT1 induction in leukocytes isolated from a new cohort of 34 breast cancer (including stage 0 patients) and 22 age-matched healthy controls and will determine if IFN defects extend to myeloid-derived cell types by interrogating IFN signaling in monocytes and possibly neutrophils (reactivity to be determined).
- We will determine the molecular basis of IFN signaling perturbations in immune cells from breast cancer patients versus healthy controls:
    - We will determine if altered expression of IFN receptors or IFN signaling pathway regulators may contribute to IFN hypo-responsiveness in cancer patients. RNA collected from peripheral blood populations will be analyzed for gene

expression using Q-PCR. Protein expression will be examined by flow-cytometry or Luminex on sorted populations.

- We will determine if altered cross-talk with other cytokine signaling pathways contributes to defective IFN-pSTAT1 signaling. Using phosflow, we will analyze STAT-phosphorylation in response to 10 cytokines including IFN-α, IFN-γ, and others which cross-talk with the IFN pathway. In addition, we will comprehensively analyze signaling pathways activated by IFN-α and IFN-γ gamma compared with IL-10 and LPS in separated monocyte and lymphocyte populations using Luminex technology. Phosphorylation of STATs 1-6, upstream JAK/TYK kinases, and the coordinately activated MAPK and NF-κB pathways will be determined.
- We will examine whether signaling pathways that lead to production of IFNs are intact in cancer patient PBMCs. We will use phosflow to assess IL-12 induced STAT4 phosphorylation, and LPS and polydA-dT:dT-dA induced TBK1 and NF-κB phosphorylation.
- If promising results are seen in our cytokine cross-talk analysis, we will determine whether suppression of the IFN pathway in breast cancer patients is a consequence of extracellular signals such as reduced IFN levels or altered cytokines that may positively or negatively cross-talk with the IFN pathway. Cytokine multiplex assays (Luminex) will be used to measure the concentrations of 37 cytokines and chemokines (including IFN-alpha), in serum from healthy vs. breast cancer patients. Cytokines showing altered expression levels that correlate with IFN pathway alterations will be selected for further examination for their potential effects on the IFN pathway.

<u>TCR and BCR signaling in breast cancer patients</u>

- Preliminary results showed a bias toward a significantly higher proportion of circulating memory T cells over naïve T cells in breast cancer patients compared to healthy controls. Moreover, preliminary analysis demonstrated that anti-CD3 induced phosphorylation of both SLP76 and ZAP70 in breast cancer naïve CD4 T cells to be reduced compared to healthy controls which could not be rescued with anti-CD3 and anti-CD28 costimulation. A total of 30 breast cancer patients and 20 age-matched healthy controls PBMCs will be assayed for Phosflow TCR signaling to confirm these current findings.
- We have observed that the proportion of memory B cells over naïve B cells in breast cancer patients is significantly lower compared to healthy controls. In addition, surface expressions of IgG and IgM showed that 95% of naive B cells expressed surface IgM in both breast cancer patients and healthy controls, indicating that the majority of these cells have not gone through antibody isotype switch, hence displaying a naïve phenotype.
- We have established that fold induction of pPLCγ2 and pERK1/2 in memory B cells in response to anti-IgG and anti-IgM stimulation was significantly reduced in breast cancer patients compared to healthy controls. However, this did not correlate with the distribution of IgM+ and/or IgG+ memory B cells in patients versus controls. In contrast, the fold induction of pPLCγ2 and pERK1/2 in naive B cells were similar between breast cancer patients and healthy controls.
- Downstream functional responses to BCR signaling are being optimized to assess the activation, apoptosis, proliferation, antibody production and cytokine secretion of circulating B cells upon BCR crosslinking. Flow-based functional assays will be used to

determine the activation (HLA-DR, CD86), apoptosis (ViViD, Annexin-V) and cell cycle progression (Vybrant DyeCycle) of purified B cells after in vitro stimulation with anti-IgM/anti-IgG for 5 days. _The supernatant will be harvested for Luminex analysis of antibody titres (IgA, IgG1, IgG2, IgG3, IgG4, IgM) and 51-plex human cytokine analysis.

Figure A1: Median expression levels of IFN-αR1 in immune cell populations of healthy controls vs. breast cancer patients. P-values of < 0.05 are indicated by *.

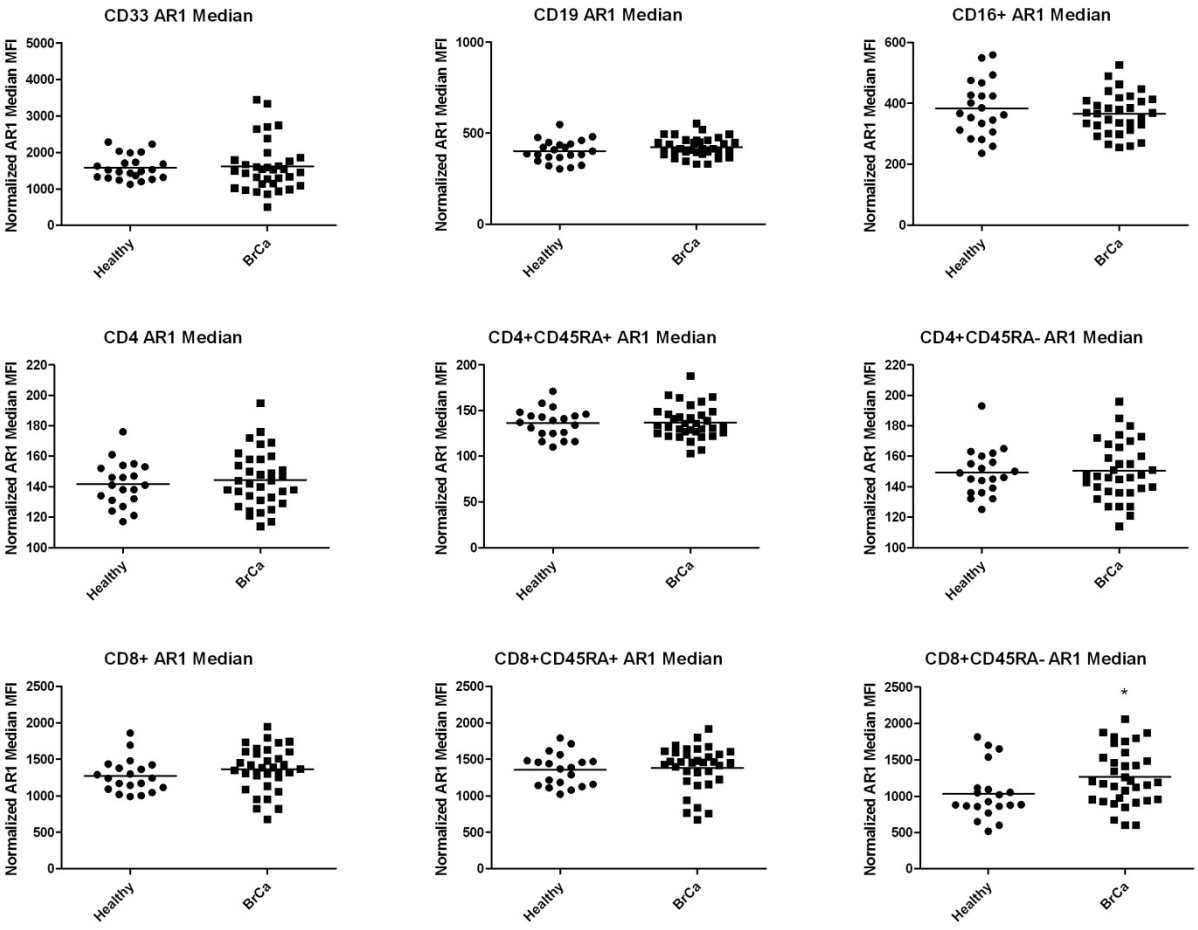

Figure A2: Median expression levels of IFN-αR2 in immune cell populations of healthy controls vs. breast cancer patients. P-values of < 0.05 are indicated by *.

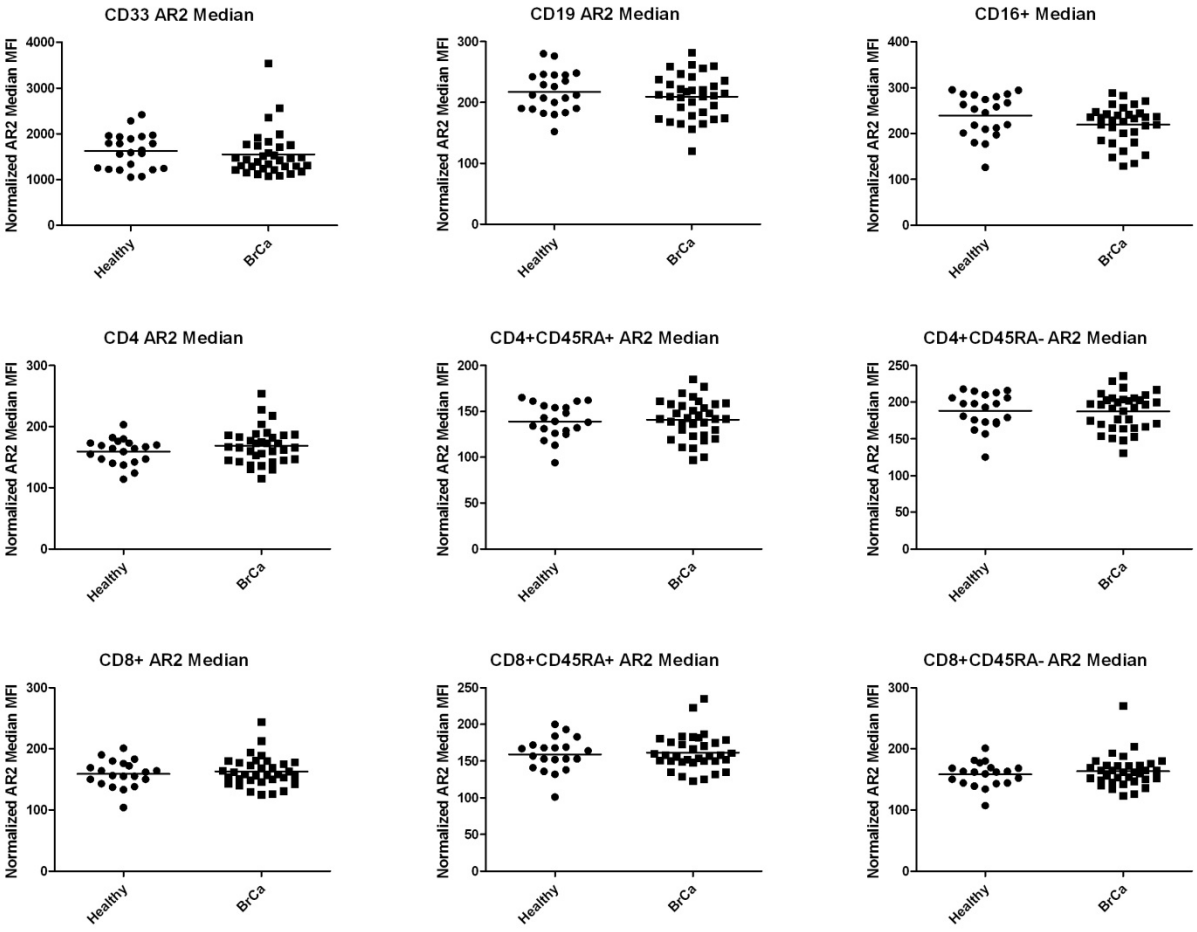

Figure A3: Median expression levels of IFN-γR1 in immune cell populations of healthy controls vs. breast cancer patients. Significant P-values are indicated by * (0.05-0.01), ** (0.001-0.01).

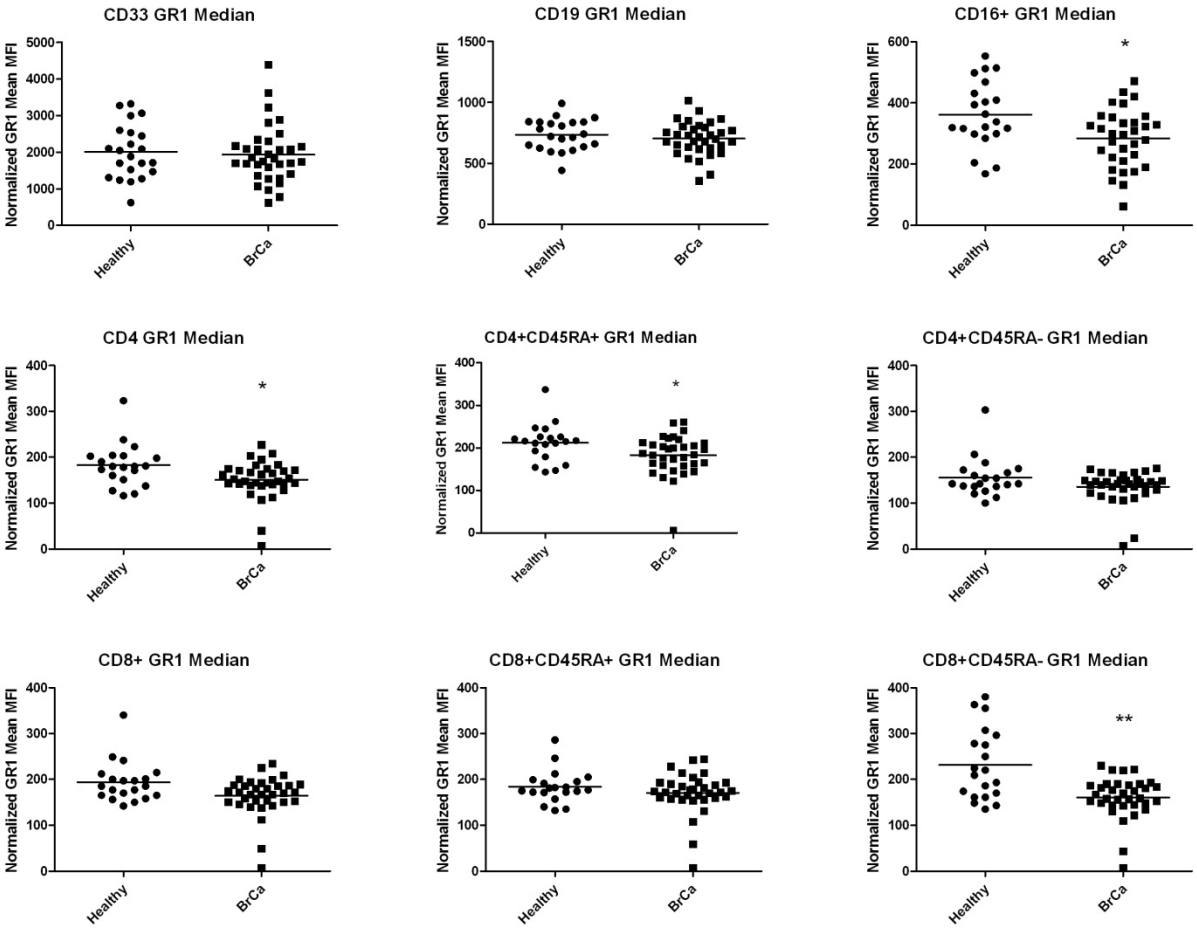

Figure A4. Preliminary data of TCR signaling Phosflow Analysis.
Preliminary data for 6 breast cancer and 7 age-matched healthy controls are presented. (a), Skewed proportion of memory T cells and naïve T cells. Y axis indicates the ratio of memory T cell percentage (CD45RA-) over naïve T cell percentage (CD45RA+). (b), Fold change in pSLP76 and pZAP70. PBMCs were stimulated with anti-CD3 and/or anti-CD28 or left unstimulated. The open circles represent cells stimulated with anti-CD3 only, and the solid circles are those stimulated with anti-CD3 and anti-CD28. The fold change of pSLP76 and pZAP70 in each T cell subset was determined by dividing the MFI of pSLP76 or pZAP70 in the stimulated cell subsets with the corresponding unstimulated subsets. Medians are indicated by the bar in each scatter column.

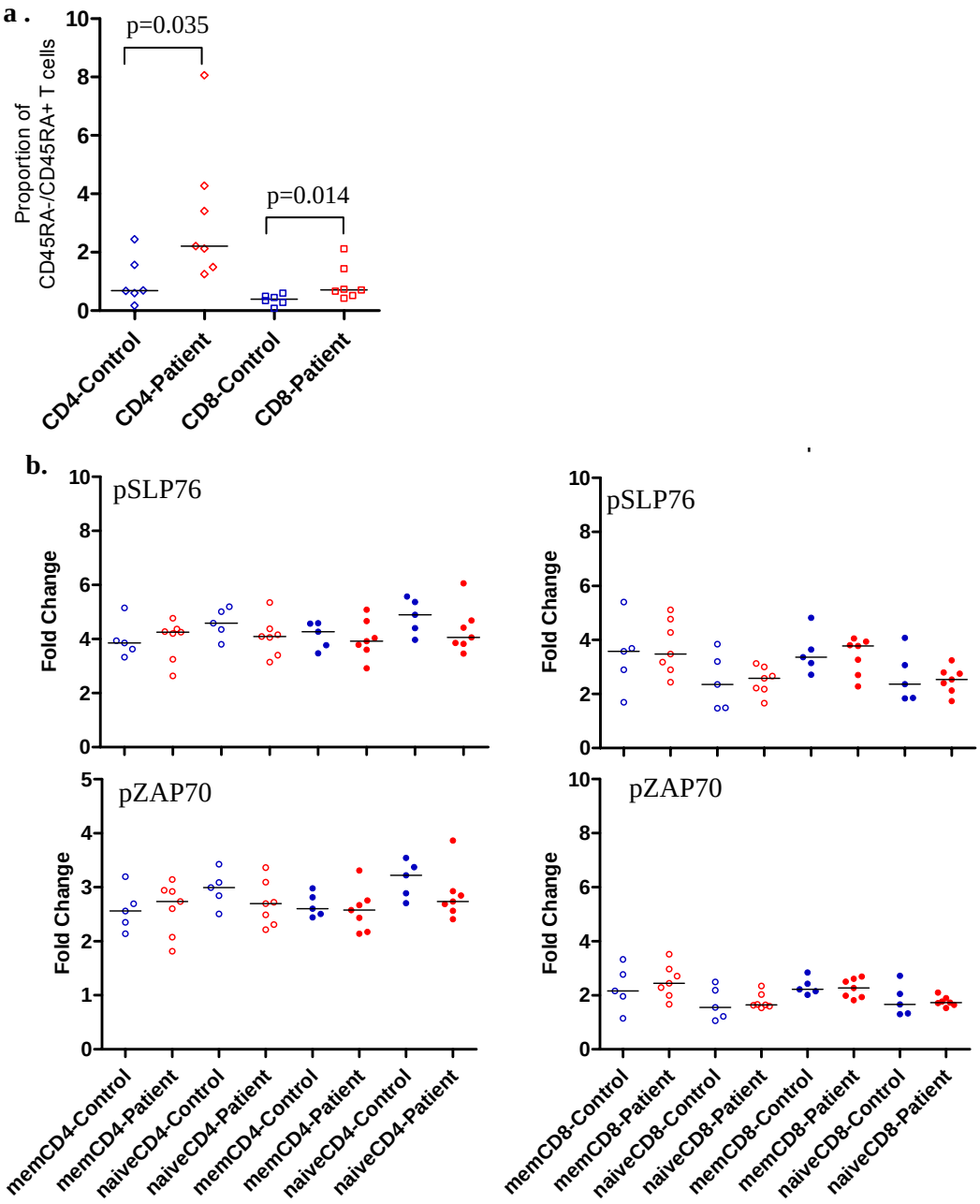

Figure A5. Altered circulating B cell Phenotype and BCR signaling in Breast Cancer Patients. (a), Skewed proportion of memory B cells and naïve B cells. Y axis indicates the ratio of memory B cell percentage (CD27+) over naïve B cell percentage (CD27-). (b), Percentage of IgG+ and/or IgM+ memory B cells, indicated by Y axis. C&D, Fold change in pPLCγ2 and pERK1/2. PBMCs were stimulated with anti-IgG and anti-IgM or left unstimulated. The fold change of pPLCγ2 and pERK1/2 in each B cell subset was determined by dividing the MFI of pPLCγ2 and pERK1/2 in the stimulated cell subsets with the corresponding unstimulated subsets. Medians are indicated by the bar in each scatter column.

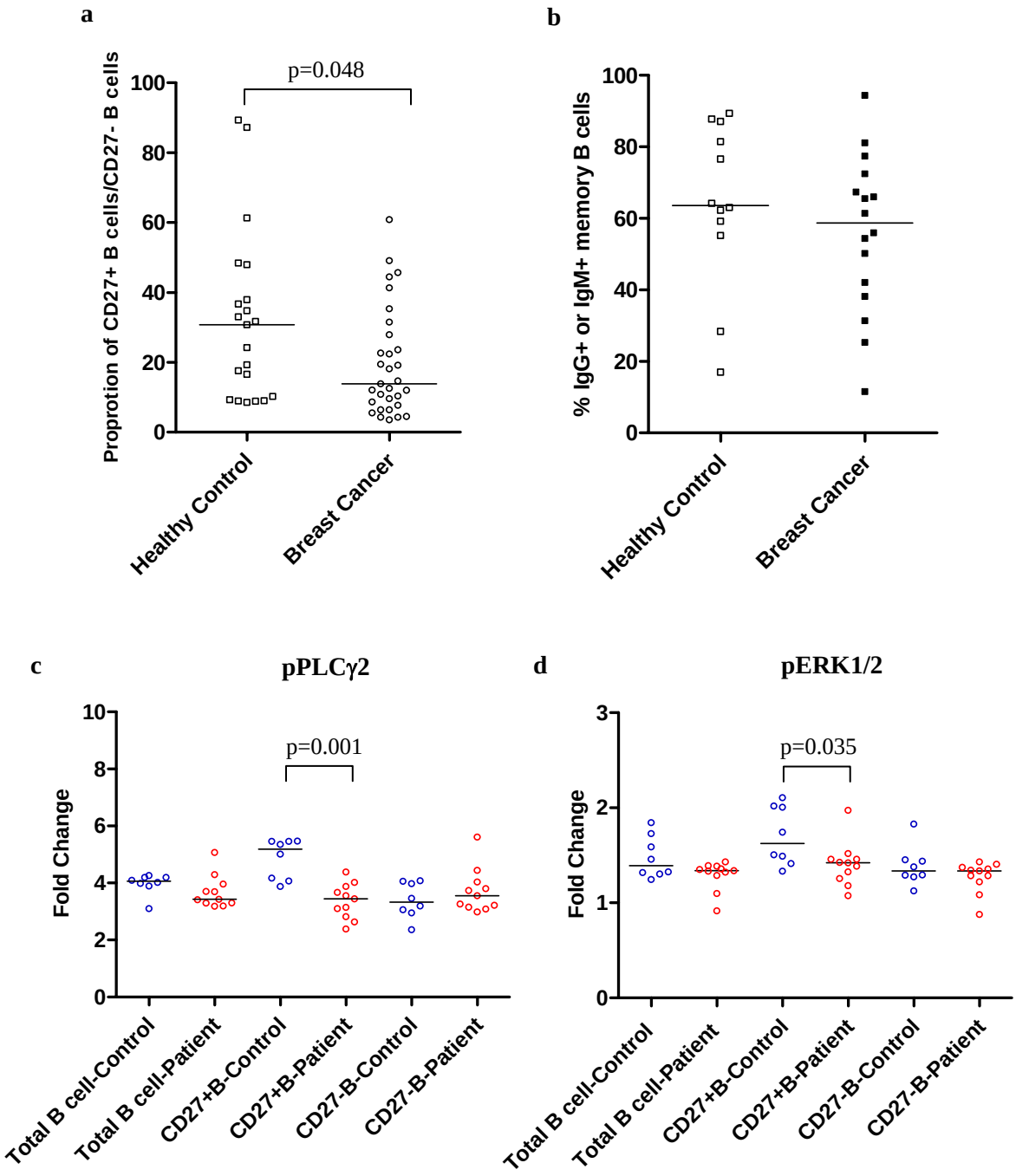

Personnel: Lee, Dirbas, Schwartz, Yu, Miyahira, Simons.

B. Microarray analysis of immune and tumor cells independently

Originally proposed in SOW:

1. Microarray analysis of gene expression of purified tumor and immune cells, isolated from fresh tumor or TDLN samples, and peripheral blood mononuclear cells (PBMC) from breast cancer patients. (months 6-60)
2. Detailed analyses of gene expression data focusing on gene networks and cross-talk between tumor and immune cells. (months 12-60)

This project utilizes a systematic approach to study the dynamics between breast cancer and the immune responses by directly comparing the gene expression patterns from TDLNs with the tumor site and peripheral blood. An increasing number of studies have used microarray to profile breast tumor specimens, which in fact represent heterogeneous cell populations consisting of tumor cells and tumor infiltrating immune cells. Our strategy is to profile purified tumor and immune cells independently, isolated from tumors and/or TDLNs.

Independent Microarray Analysis of Immune Cells and Tumor Cells

Key accomplishment for year 4 includes the completion of a second batch microarray experiment and a more in-depth analysis of the complete microarray data set. This led to several key findings including lymphocyte dysfunction and expansion of tumor-promoting myeloid cells in breast cancer patients' blood and tumor draining lymph nodes (TDLNs). Aside from the immune dysfunctions, a Polycomb repression signature was identified in metastatic tumor cells isolated from TDLNs and showed higher expression compared to primary tumor cells.

Summary of the sample composition of the microarray data set

We took an integrative systems approach to study the dynamics between breast cancer and the immune responses by directly comparing the gene expression patterns between tumor, TDLNs, and PBMCs. The first set of patient specimens comprise of 156 samples collected from 24 breast cancer patients. However, the immune cell composition and function in each anatomical compartment is very different. To differentiate true cancer-associated immune dysfunctions from anatomical compartment associated signatures, we have been collecting healthy peripheral blood specimens and non-cancer lymph nodes for microarray data analysis. Unfortunately, the acquisition of non-cancer lymph nodes has been extremely difficult and it is almost impossible to obtain normal lymph nodes. Therefore, the second batch microarray included ten peripheral blood specimens from age and gender matched healthy donors, five non-cancer lymph nodes from one inflammatory bowel disease patient and one normal lymph node RNA from an aortic aneurism patient. In addition to the control samples, another 24 samples from 6 breast cancer patients were included in the second batch gene expression profiling.

Tumor-induced lymphocyte dysfunction in Breast Cancer TDLNs

TDLNs undergo profound immune alterations due to the upstream tumor. Preliminary analysis of the initial set of microarray data showed up-regulations of cell cycle checkpoint pathways and TGF-β pathway in TDLNs compared to PBMCs. We hypothesized that clonal expansion of lymphocytes in TDLNs are blunted due to processes initiated by the upstream tumor.

A. Validation through immunohistochemical staining of TDLNs sections

To validate the microarray array data, we optimized a 4-color immunohistochemical (IHC) staining panel to assess the lymphocyte proliferation status in breast cancer TDLNs. Ki67 is a proliferation marker expressed by proliferating cells in all phases of the active cell cycle (G1, S, G2 and M phase) and absent in resting (G0) cells. In addition to Ki67, we also selected a panel of antibodies directed against cells of interest: CD3 T cells, CD20 B cells, AE1/AE3 for tumor cells. Images are acquired using the automated imaging system (Olympus and Ludl) with Nuance™. Acquired images are then analyzed with our custom image analysis software GemIdent to identify and enumerate the following phenotypes: T cells, B cells, tumor cells, Ki67+ T cells, Ki67+ B cells, Ki67+ tumor cells. The number of Ki67+ T cells divided by the total T cell number represents the percentage of proliferating T cells. The number of Ki67+ B cells divided by the total B cell number represents the percentage of proliferating B cells. A total of 23 breast cancer lymph nodes, 10 non-cancer reactive lymph nodes and 6 normal lymph nodes were stained and analyzed (Figure B1**)**.

Both breast cancer TDLNs and normal LNs showed significantly lower percentages of proliferating T cells than non-cancer reactive LNs. However, T cells from breast cancer TDLNs have a similar proliferating capacity compared to normal lymph nodes, suggesting a resting or anergic T cell phenotype in the breast cancer TDLNs. Further stratification of samples according to tumor involvement, patients' stages, or sentinel lymph node (SLN)/non-sentinel lymph node (NSLN) showed no significant differences (Figure B2).

On the other hand, the proportion of proliferating B cells from breast cancer TDLNs was significantly higher than normal lymph nodes, and lower than non-cancer reactive lymph nodes suggesting differential B cell responses against tumor antigen occur in breast cancer TDLNs. Further stratifications according to tumor involvement, patients' stages, or sentinel lymph node (SLN)/non-sentinel lymph node (NSLN) showed no significant differences (Figure B2). Of particular interest, germinal center (GC)-like structures are often observed in heavily tumor infiltrating lymph nodes and are surrounded by tumor cells. These GC-like structures are comprised of highly proliferating B cells and an increased proportion of T cells, with the loss of both mantle zone and GC polarization (Figure B3). We hypothesize that B cells in breast cancer TDLNs are responding to tumor antigens even after tumor cells metastasize to TDLNs. However, these responding B cells in the TDLNs will eventually be eradicated when tumor progressively takes over TDLNs.

Tumors might have evolved different strategies to induce T cell and B cell dysfunction in TDLNs. Induction of T cell tolerance may occur before tumor metastasizes to the lymph nodes and prepare lymph nodes for tumor metastasis. Currently it is unknown whether B cell responses are blunted in the early stage of tumor development. Further staining of key players for B cell

responses is being performed to answer these questions. These include markers to stain for follicular dendritic cells, follicular T helper cells, histiocytes and apoptotic cells.

B. Microarray Data: Breast Cancer TDLNs compared to non-cancer Lymph Nodes

Further analysis of the second batch of microarray data using Gene Set Enrichment Analysis (GSEA) confirmed the first batch findings of an up-regulation of cell cycle arrest pathways (ATM pathway, ATRBRCA pathway, G2 pathway) in breast cancer TDLNs compared to non-cancer lymph nodes. Three anergy-related genes are significantly higher in breast cancer TDLNs compared to non-cancer lymph nodes:

- PD1, an inhibitory molecule expressed on T cells, contributes to T cell tolerance ($p=0.0036$)
- CDC14A, controls cell cycle and is associated with T cell anergy ($p=0.00016$)
- CBL, negatively regulates T cell signaling ($p=0.0071$)

Quantitative PCR are currently being carried out to validate these findings. If this holds true, functional analysis of T cells from breast cancer TDLNs will be carried out to assess T cell activation, proliferation and apoptosis.

<u>Tumor-induced Expansion of Tumor-promoting Myeloid Cells in TDLNs</u>

Tumor tissues are often infiltrated by a heterogeneous set of myeloid cells: macrophages and neutrophils, myeloid derived suppressor cells (MDSCs), and tolerized dendritic cells. These cells promote tumor growth by producing soluble mediators (VEGF, MMPs, TGF-β etc), inducing regulatory T cells and leading to effector T cell dysfunctions.

Intriguingly, microarray analyses of breast cancer TDLNs with non-cancer lymph nodes revealed an upregulation of signatures associated with tumor-promoting myeloid cells in the breast cancer TDLNs. Arginase 1 (ARG1), generally expressed by tumor-promoting myeloid cells is increased in breast cancer TDLNs compared to non-cancer lymph nodes ($p=0.015$). The increased expression of Arginase 1 is positively correlated with patient stages but not with tumor metastasis in the lymph nodes. Apart from ARG1 expression, oncostatin M (OSM) and matrix metallopeptidase 9 (MMP9) showed significant increased expressions in breast cancer TDLNs as well ($p=0.0003$; $p=0.027$). Oncostatin M promotes tumor metastasis and angiogenesis by upregulating VEGF. MMP-9 is known as the 92-kDa type IV collagenase/gelatinase, which implies that MMP-9 can degrade basement membranes, the initial step in carcinoma invasion. Both oncostatin M and MMP9 are expressed mainly by myeloid cells and often highly expressed in tumor tissues.

We hypothesize that tumor cells hijack ‘a protective acute inflammatory process’ mediated primarily by myeloid cells to prepare TDLNs to become a privileged site for tumor metastasis. This process might be initiated by the upstream tumor remotely and/or involve recruitment of these tumor promoting myeloid cells from other compartment such as bone marrow, blood, and/or tumor tissues to the TDLNs. The local tolerance in TDLNs is then intensified by self-amplifying mechanisms which contributes to systemic tolerance and further tumor progression. Currently, quantitative PCR are being carried out to validate the differential expression of Arginase 1, oncostatin M and MMP9 in TDLNs. Expression of these genes will also be

quantified in peripheral blood to determine whether the expansion of tumor-promoting myeloid cells is systemic and/or offers prognostic information.

The Polycomb Repression Signature in Metastatic Tumor Cells from Breast Cancer TDLNs

Upregulation of the Polycomb repression signature was observed in metastatic tumor cells isolated from TDLNs compared to primary tumor lesions through network analysis. Polycomb group (PcG) proteins are transcriptional repressors and play a central role in epigenetic silencing target genes. The PcG proteins EZH2, SUZ12, EED, RBBP4 form the polycomb repressive complex 2 (PRC2) and are significantly increased in metastatic tumor cells compared to primary tumors. Dysregulation of PRC2 proteins in epithelial cells or tumor cells may lead to silencing of tumor suppressors and metastasis suppressors and promotes neoplastic transformation and tumor metastasis.

Correlation analysis of the tumor cell microarray data is being carried out to search for novel tumor suppressors and metastasis suppressors targeted by PcG proteins through epigenetic silencing. Analysis of PRC2 chip-on-chip and chip-seq data from GEO will also be performed to evaluate whether these are potentially the target genes. Quantitative PCR will then be carried out to confirm the differential expression of PRC2 proteins EZH2, SUZ12, EED, RBBP4 and their targets in metastatic tumor cells from TDLNs and primary tumor cells. Over expression of PRC2 proteins and knockdown of PcG proteins in breast cancer cell lines will be used to further validate these targets.

Figure B1. IHC analysis of Proliferating Lymphocytes from Breast Cancer and Control Lymph Nodes. A total of 23 breast cancer lymph nodes, 10 non-cancer reactive lymph nodes and 6 normal lymph nodes were stained and data is presented in separate scatter columns. Y axis indicates the percentage of proliferating T cells (1a) and proliferating B cells (1b). Medians are indicated by the bar in each scatter column. P-values < 0.5 were considered significant.

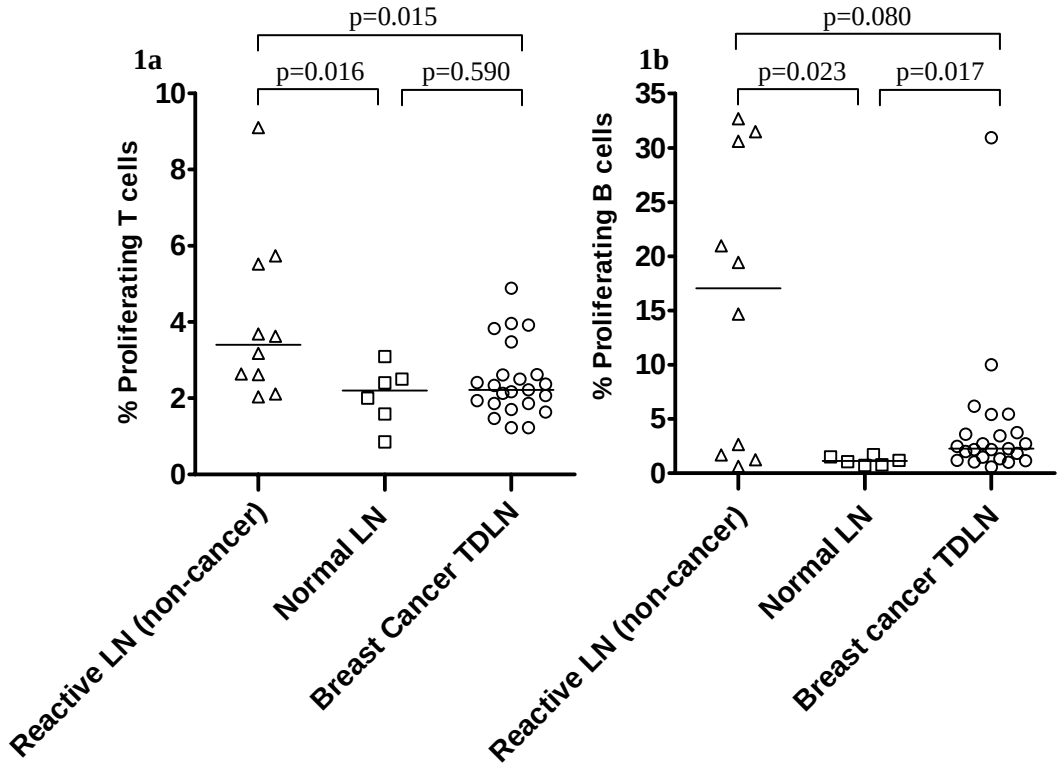

Figure B2. IHC analysis of proliferating T cell and B cell proportions in Breast Cancer TDLNs: Stratified by Tumor involvement, patients' stages, and sentinel/non-sentinel lymph nodes (SLN/NSLN, respectively).

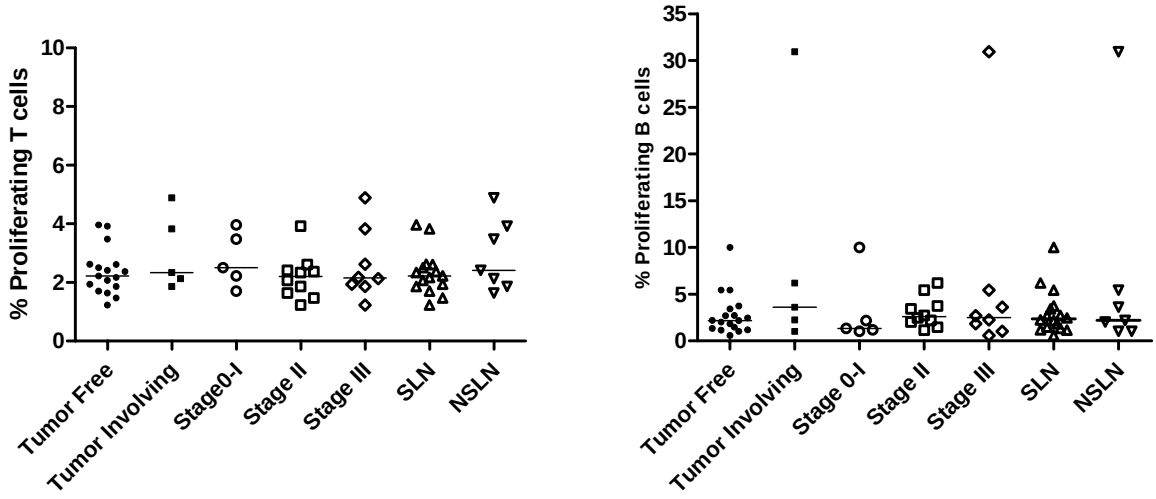

Figure B3. Germinal Center (GC)-like Structures in Tumor positive Lymph Nodes. The images were presented in pseudo-colors: Ki67-green nuclear, B cells-red membrane, T cells-blue membrane, Tumor cells-purple membrane.

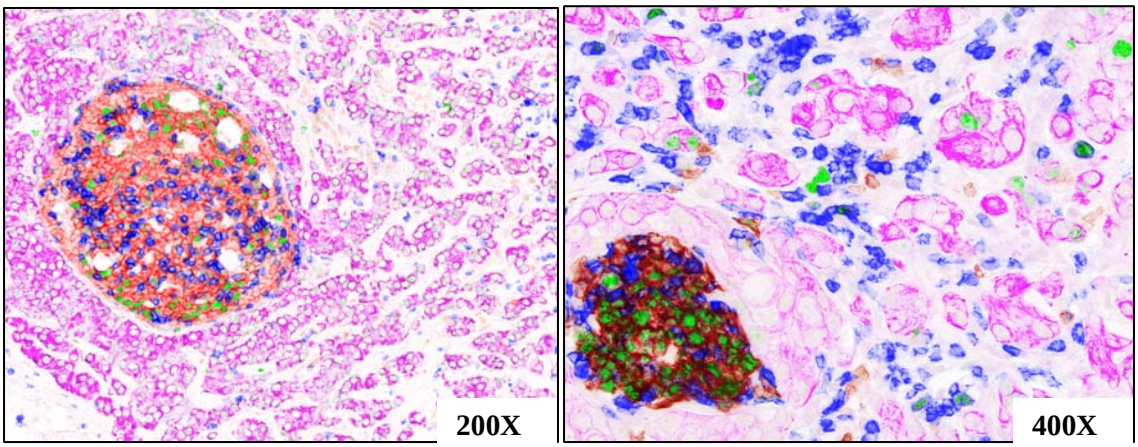

Personnel: Lee, Holmes, Dirbas, Yu, Simons. **A third PhD postdoctoral fellow with expertise in bioinformatics, data integration and analysis would greatly enhance the success of this project.**

C. Analyzing the geometric relationships and interactions between cancer and immune cells in tumors and TDLN

Originally proposed in SOW:
1. Generate high-resolution images of tumor and TDLN sections. (months 0-60)
B. Develop algorithms to identify cells/cell types and assign coordinates. (months 0-60)
2. Develop algorithms to assess the spatial arrangement and grouping of tumor and immune cells with respect to each other that may have biological significance. This will be done in collaboration with a Stanford mathematics professor, Dr. Doron Levy, using advanced image analysis and computational geometry techniques. (months 0-60)

Data from archived samples of tumor and TDLN from breast cancer patients with 1-13 years of clinical follow-up are being analyzed. To date, we have acquired samples from a total of 63 breast cancer patients treated at Stanford Medical Center in 1997-2004, 16 from Vermont University Hospital in 1994-1995, and 5 from Memorial Sloan Kettering Cancer Center in 2000. As control samples, we have obtained healthy intramammary and axillary lymph nodes (HLNs) from 7 patients who had prophylactic mastectomy or breast reduction surgery at Stanford Medical Center in 2001-2007.

Tumor and immune cell markers are identified via immunohistochemical staining (IHC), immunofluorescence (IF) staining, and in-situ hybridization (ISH). Images are being acquired using a high-resolution, automated imaging system with a special spectral imaging system (Vectra^{TM}). Acquired images are then analyzed with our custom image analysis software GemIdent. This software uses spatial statistics and machine learning algorithms to identify cells, cell types, and assign coordinates. We are also developing algorithms to assess the spatial arrangement and grouping of tumor and immune cells. By performing *in situ* analysis of tissue, our goal is to understand the mechanisms of cancer development by characterizing the spatial interactions between cell types. This is done in collaboration with Stanford statistics professor, Dr. Susan Holmes, who has expertise in novel image analysis and computational geometry techniques. Over 50 immune and tumor markers will eventually be assessed within tumor and TDLN sections.

Our key accomplishments in year 4 include optimization of up to 5-color IHC staining combinations to concurrently visualize breast cancer cells (via cytokeratin AE1/AE3), T cells, B cells, mature and immature myeloid dendritic cells (DCs) within TDLN sections (Figure C1). We have also optimized other multi-color staining combinations to analyze other immune cell populations, such as CD4 and CD8 T cells, T-regulatory cells (T-reg) and plasmacytoid DCs (pDCs). We have fully integrated our four-staged image analysis approach incorporating 1)

multi-dimensional tissue staining, 2) high-resolution, automated whole-section imaging, 3) custom image analysis software that identifies cell types of interest, and 4) numerical and spatial statistical analysis, such as cell densities, distances, and distribution patterns.

Quantification of CD3+ T cells, CD20+ B cells and CD1a+ dendritic cells (DCs) and analyses of their relationship with clinical parameters and outcomes.

To date, we have been concentrating our study using TDLN samples from patients with a tumor positive SLN (SLN+) dissection. Using pairs of tumor-invaded (+) and tumor-free (-) NSLNs (NSLN+ and NSLN-) from 10 patients, we found that the DC proportion was generally lower in NSLN+ samples (p=0.03) (Figure C2a). This trend was also observed in B cells (Figure C2b), although not significant with the current sample size (p=0.08). In contrast, this trend was not observed in T cells (p=0.3) (Figure C2c).

DC proportions in SLN+, NSLN+ and NSLN- were found to be lower than in HLNs (Figure C3b), indicating that cancer development depleted DC populations in the TDLNs and, interestingly, was independent of tumor invasion status. The median value of DC proportion in tumor-free NSLNs was determined to be similar, regardless of NSLN dissection (NSLND) status (Figure C3a). Furthermore, we found that DC maturation is also impaired in breast cancer TDLNs. The number of mature DCs was particularly lower in tumor-invaded NSLNs compared to tumor negative NSLNs (Figure C4a). In 4 out of 5 pairs of NSLNs analyzed, the proportion of mature DCs in tumor negative NSLNs was higher compared to tumor-invaded NSLN pairs (Figure 4b). Further analysis showed the proportions of overall DCs, mature DCs, T cells and B cells were found to be similar in patients with different clinical outcomes (Figure C5).

<u>Proportions of T cells and B cells in SLNs, NSLNs, and HLNs</u>

Proportion of CD3+ T cells was lower in both tumor-invaded NSLNs and tumor free NSLNs from NSLND+ patients compared to NSLNs from NSLND- patients (Figure C6a). Though not significant, the median values of T cell proportion from NSLND+ patients showed the same trend compared to HLNs. The proportion of T cells and B cells was found to be similar in SLNs+, NSLNs+ and HLNs (Figure C6b and Figure C7, respectively). We then correlated the T cell and DC proportions with various clinical parameters. We found that NSLNs- from patients with stage III disease and were NSLND- tended to display lower T cell proportions compared to other NSLNs- from patients with earlier stages of disease (Figure C8). No significant difference in DCs proportion was observed in NSLNs from patients with different stages of cancer. With the current sample size, we also did not observe significant differences in both T cell and DC proportions in groups of NSLNs from patients with different Her-2 status, breast cancer subtypes, tumor grades and angiolymphatic invasion status (Figure C9 - C12). We have yet to correlate the proportions of B cells and DC maturation with different clinical parameters.

Spatial analysis of the Distribution of T cells and B cells

At present, we have analyzed T cell and B cell distributions in tumor-invaded SLNs from 15 breast cancer patients (1 SLN per patient) treated at Stanford University Medical Center in 1997-2003 and in 7 HLN controls. These samples were subjected to our four-staged image analysis approach (Figure C13). The data obtained by GemIdent analyses are the coordinates and

antibody labels of a large number of points. These form a marked spatial point process that we analyzed using standard spatial statistics [Baddeley, *et al*., 2005; Diggle, P. J., 2003]. Ripley's K function is a method for analyzing point process data [Dixon, P.M., 2002]. In our study, we used the L function, a variance stabilized version of the K function, which allowed us to detect deviations from spatial homogeneity [Dixon, P.M., 2002]. Our theoretical target distribution was the inhomogeneous point process made by T cells, and we tested whether B cells followed a similar clustering process as T cells.

To get a better understanding of the distances between cells, we computed a distance matrix using 500 B cells which were randomly selected from a lymph node section. We computed 500*500=250,000 inter-point distances and found that the minimum distance of a B cell to its nearest neighbor was 11 units of radius, and the maximum was 745. Interestingly, we found that in 5 out of 7 (71%) HLNs, B cells had a similar tendency to cluster at various distances as T cells within the same tissue section, indicated by the L function of the B cells that remained within the confidence envelope of the T cells (Figure C14a-b). This was not the case in most of the tumor-invaded SLNs, in which the L function of the B cells was similar to that of the T cells in 5 out of 15 (33%) nodes. In all cases where the L function of the B cells deviated away from the confidence envelope made by the T cells, the line deviated above the envelope, indicating that B cells were clustered together more than T cells (Figure C15a-b).

In order to confirm the validity of our L function tests, we compared the L function of tumor cells with that of T cells. Results from all tumor-invaded SLNs showed that the L function of the tumor cells fell below the envelope of the T cells (Figure C16) indicating tumor cells' nuclei were further apart from each other compared to T cells' nuclei within a section of a lymph node. These results were expected since we could grossly observe that tumor cells were larger and had thicker membranes than T cells and, therefore, their nuclei could not be physically closer to one another. In addition, we determined there to be no correlation between the amount of tumor burdens of the SLNs and the similarity or discrepancy between the L functions of the T cells and B cells.

We then simulated the time spent by the L functions of B cells outside of the T cells envelope between 0 to 500 units of radius. We observed that 9 out of 15 L functions of the B cells in the SLNs+ and 1 out of 7 in the HLNs exited the T cells' envelopes in radii below 150 (Figure C17). At a radius of 150, the average time of the L functions of the B cells from SLNs+ spent outside of the envelope was 8.9, while it was 1.6 for the B cells from the HLNs ($p=0.02$).

The mechanism that causes the discrepancy in the T and B cells spatial distribution that was newly discovered in the majority of the tumor-invaded SLNs is unknown at this stage and requires further investigation. We will expand this investigation using pairs of tumor-invaded and tumor-free lymph nodes to determine whether or not this happens as a result of tumor invasion into the lymph nodes. Furthermore, we will investigate any correlation with various clinical parameters and disease outcomes.

Figure C1. An RGB image of a TDLN cross section taken by Vectra^{TM} at 200x maginification. Chromogens used were Bajoran Purple (cytokeratin (tumor), purple), AEC (CD20 B cells, orange, (pseudo-colored brown)), Ferangi Blue (CD3 T cells, dark blue), Vulcan Red (CD1a DCs, red) and DAB (CD83 mature DCs, brown (pseudo-colored green)). Cellular nuclei were counterstained with hematoxylin (light blue).

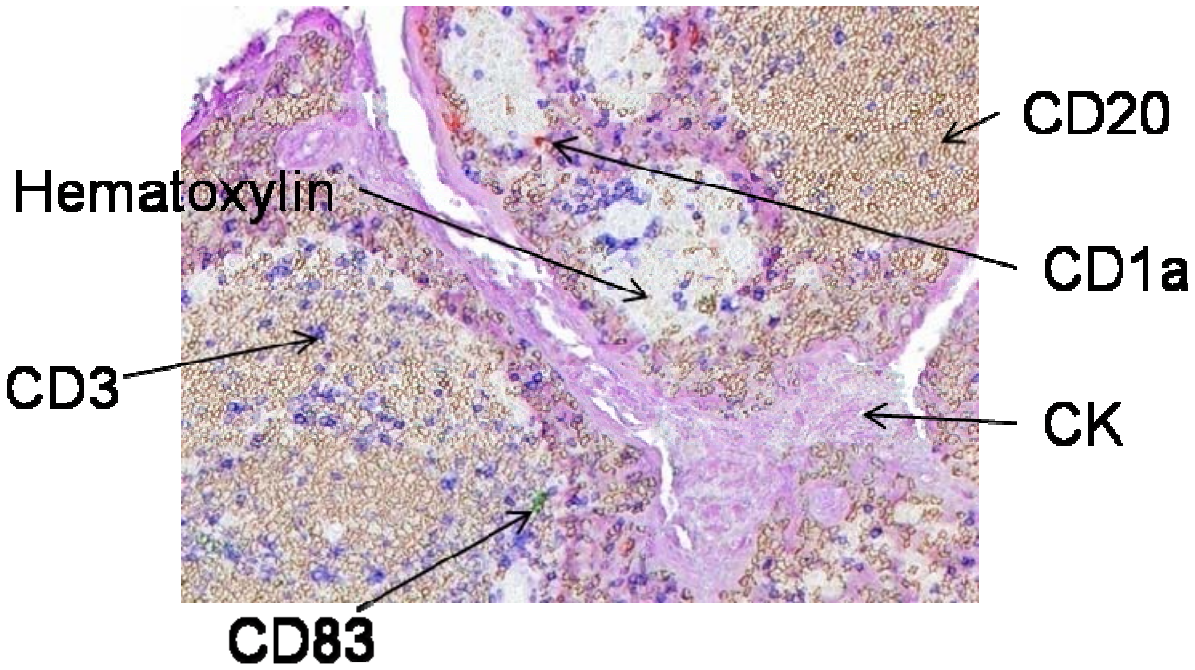

Figure C2. Analysis of a) DCs, b) B cells and c) T cell proportions in pairs of tumor-invaded and tumor-free ALNs (NSLNs) (n=10; *p<0.05).

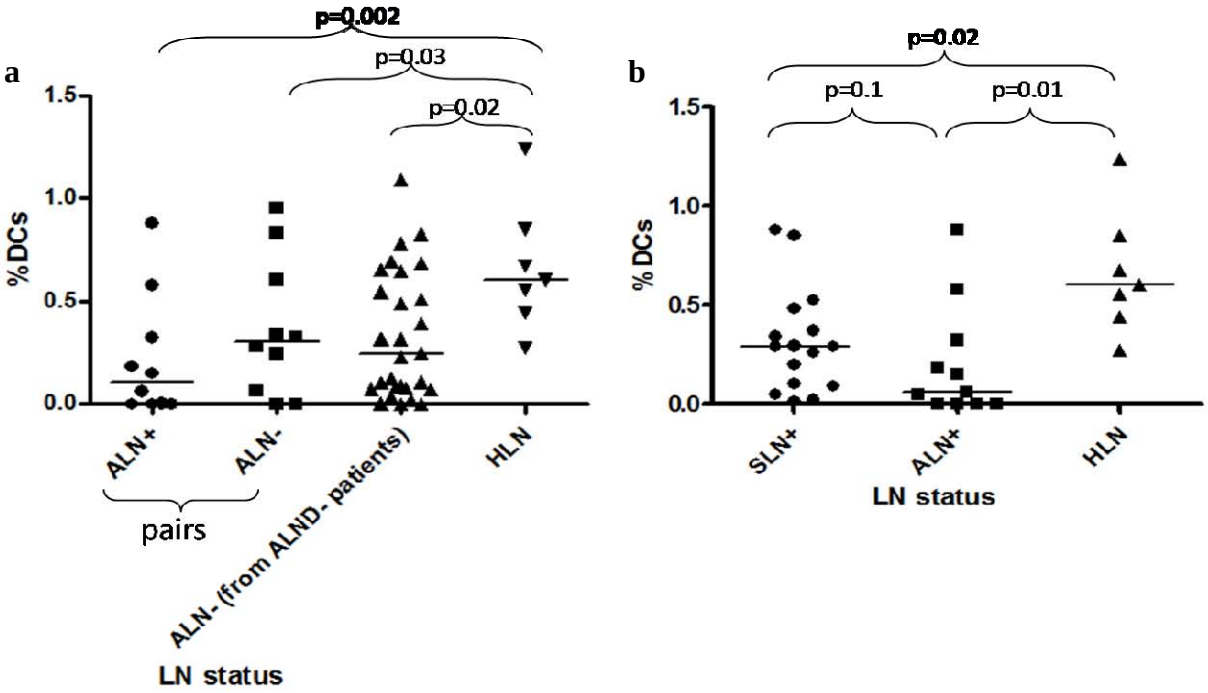

Figure C3. DC proportion is reduced in breast cancer TDLNs, particularly in tumor-invaded NSLNs (ALN).

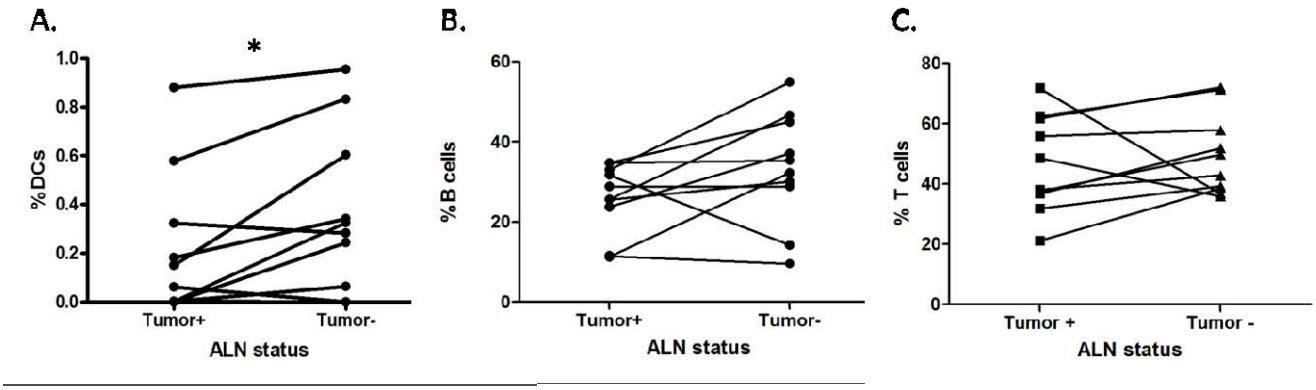

Figure C4. a), DC maturation is impaired in BrCa TDLNs. b), Proportions of mature DCs are generally higher in tumor-free ALNs compared to the tumor-invaded pairs.

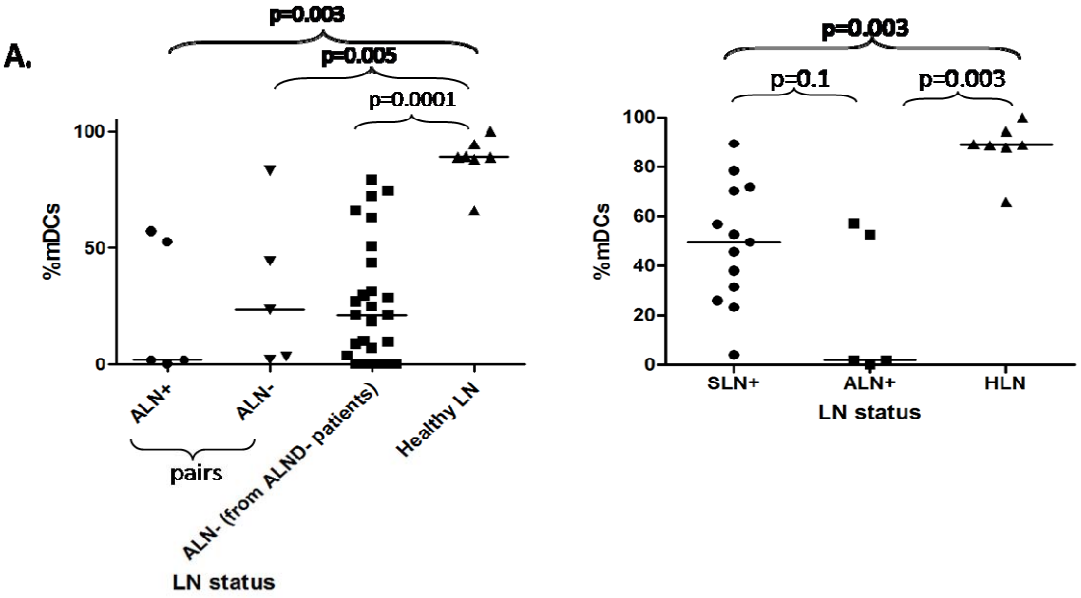

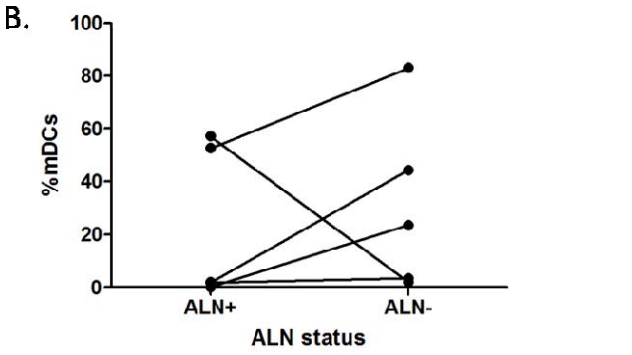

Figure C5. Proportions of overall DCs, mature DCs, T cells and B cells are similar in disease-free (DF) and relapsed (Rel) patients.

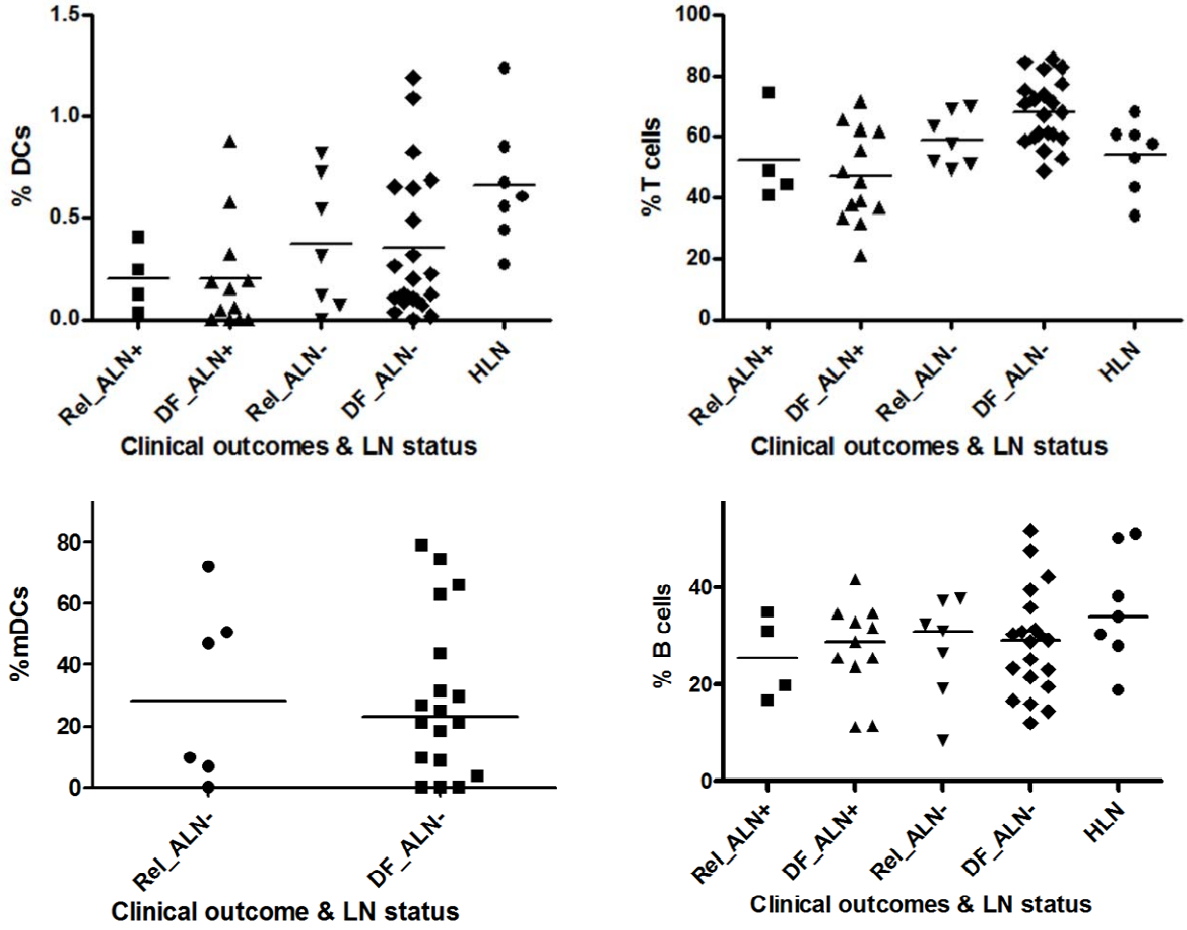

Figure C6. T cell proportion decreases in ALNs (NSLNs) from patients with tumor-involved NSLN disections

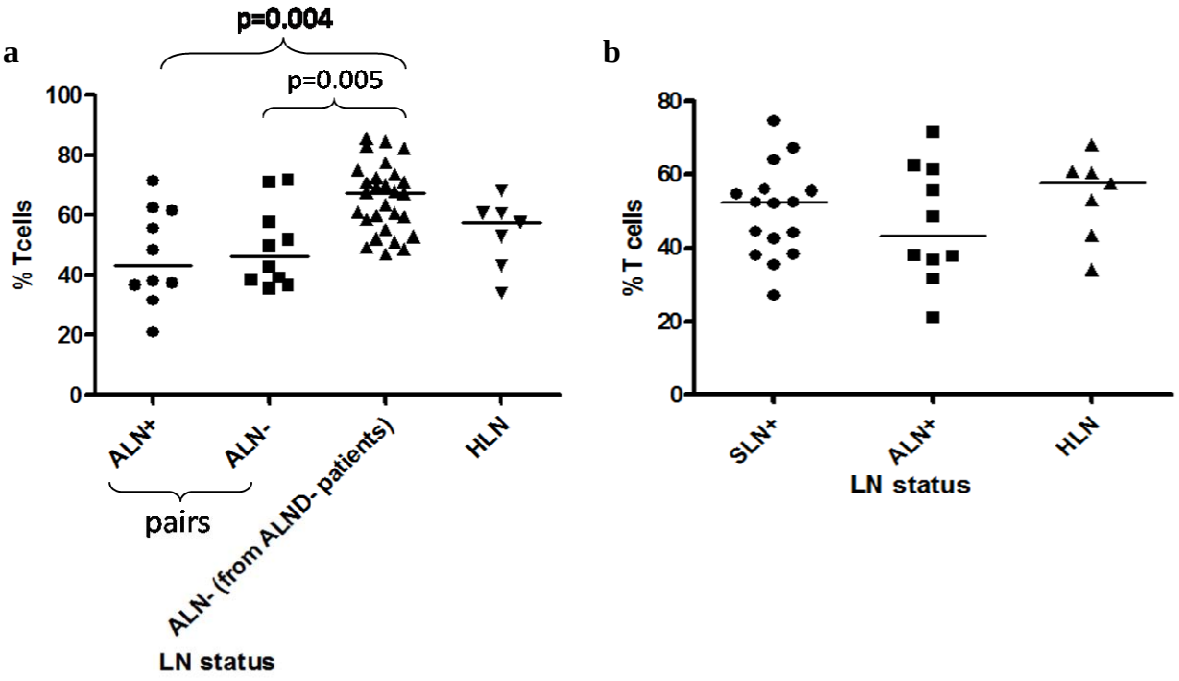

Figure C7. B cell proportion is similar in SLNs, ALNs and HLNs.

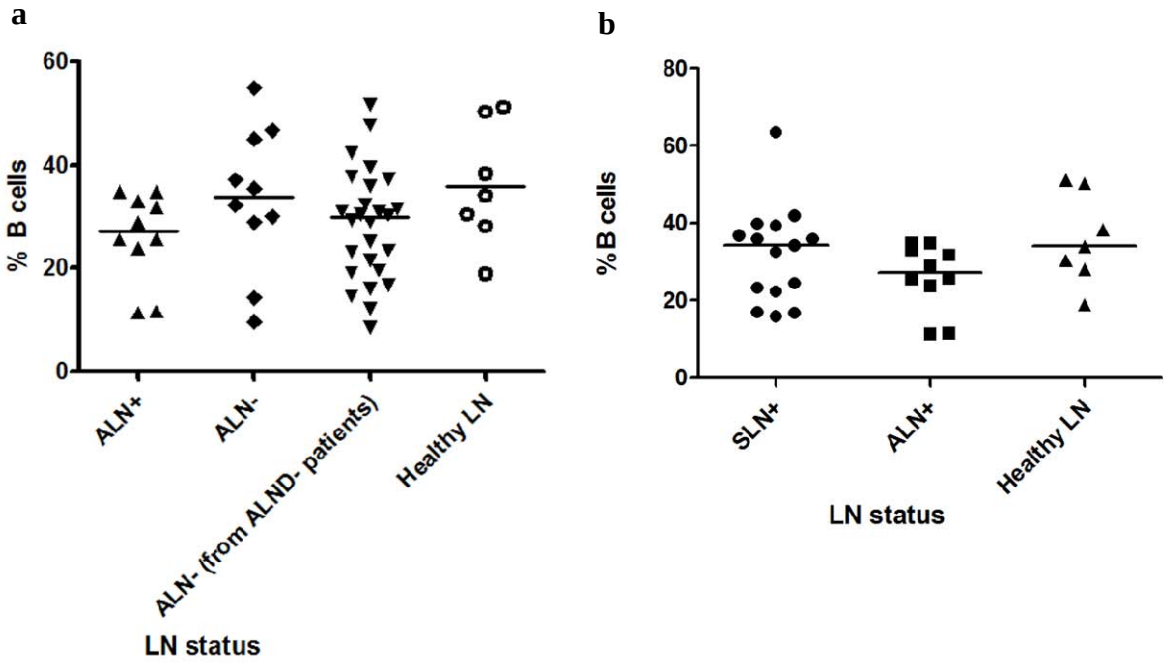

Figure C8. Proportions of DCs and T cells in ALNs (NSLNs) from patients with different stages of breast cancer *p<0.05.

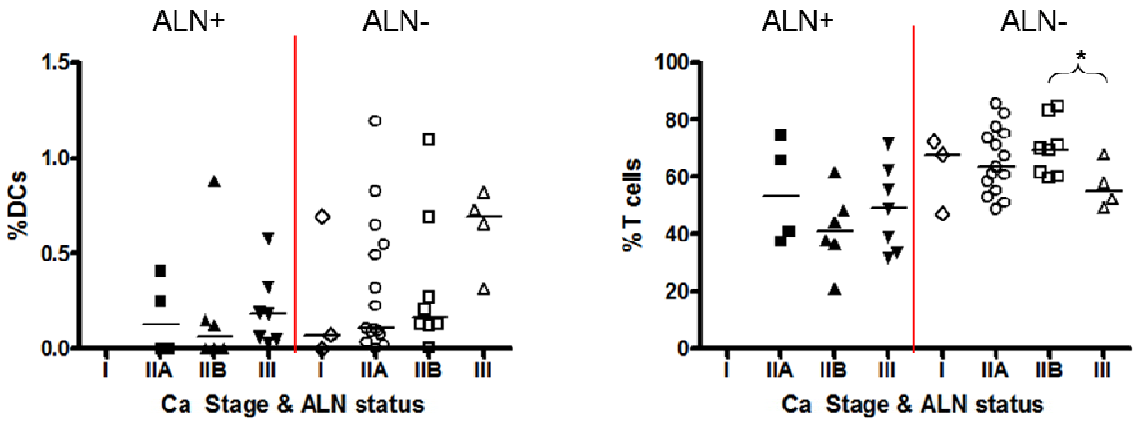

Figure C9. Proportions of DCs and T cells in ALNs from patients with or without overexpression of Her-2 in primary breast tumors.

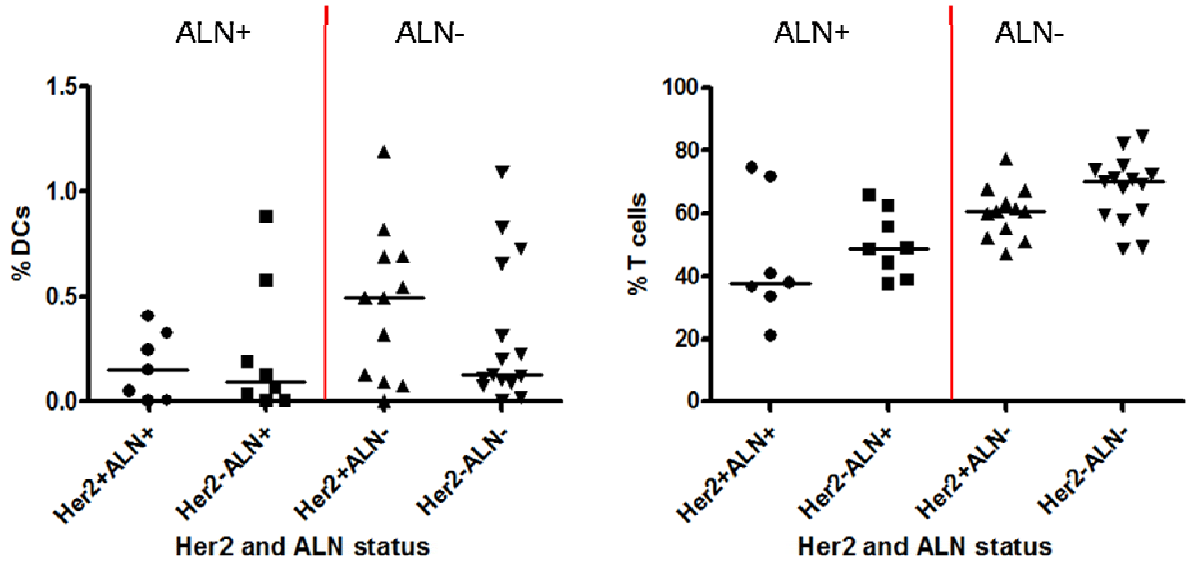

Figure C10. Proportions of DCs and T cells in ALNs (NSLNs) from patients segregated by breast cancer subtypes: basal, luminal A, luminal B and Her-2.

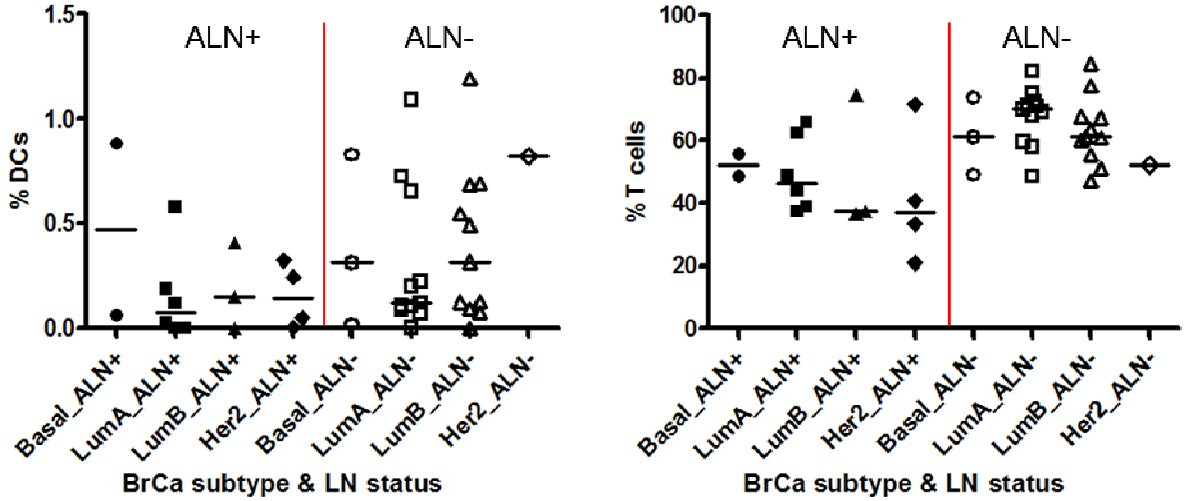

Figure C11. Proportions of DCs and T cells in ALNs from patients segregated by primary tumor grade.

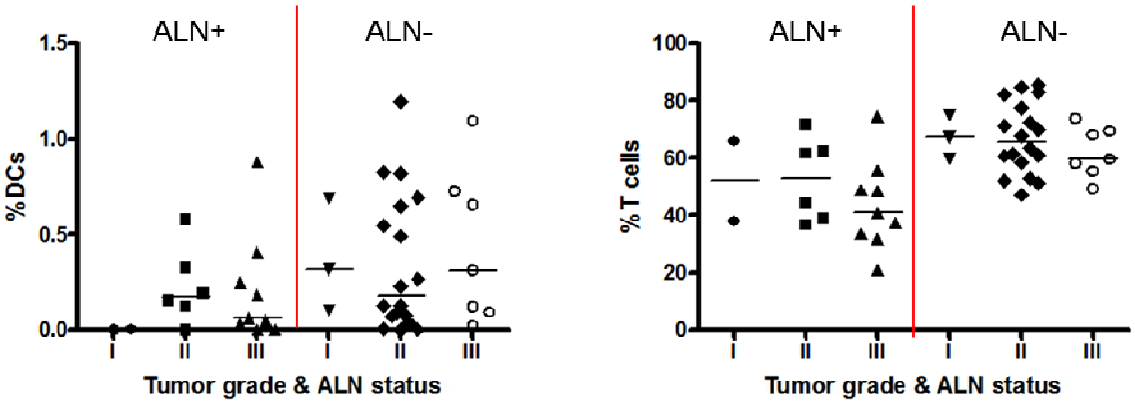

Figure C12. Proportions of DCs and T cells in ALNs from patients with the presence (+) or absence (-) of angiolymphatic invasion.

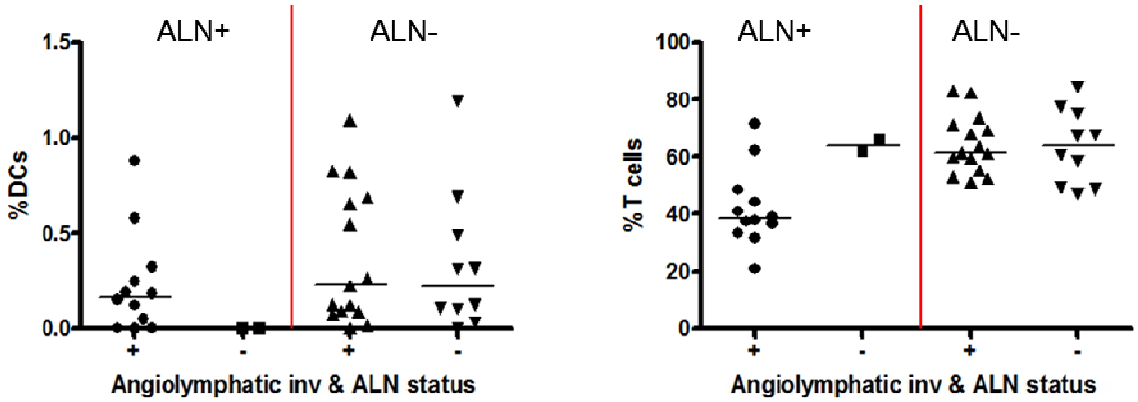

Figure C13. Integrated image analysis approach. Stage 1: multicolor staining of tissue sections. Stage 2: high-resolution spectral imaging and automated scanning of the whole tissue section. Stage 3: machine-learning-based cell identification by GemIdent. Stage 4: numerical and spatial statistical analyses, such as cell densities, distances and distribution patterns.

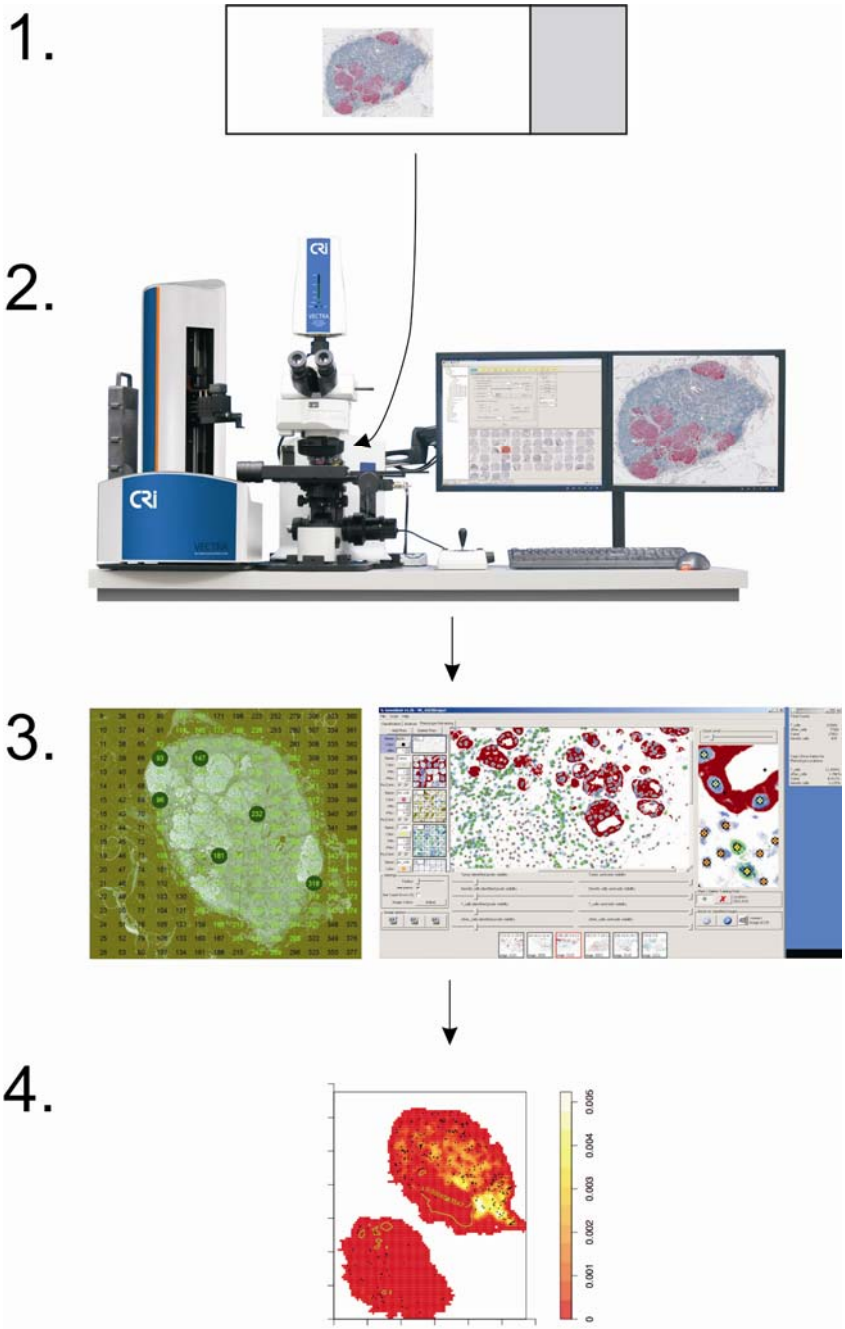

Figure C14. Representative graph and images of spatial distribution of B cells that is similar to T cells. a), The L function of B cells, indicated by the solid line, remained inside the confidence envelope (indicated by the light-blue and dark-blue dotted and dash lines, respectively) of T cells. b), Image of T cell and B cell distribution on a lymph node cross section, showing a similar tendency of the T cells and the B cells to clump or disperse.

a

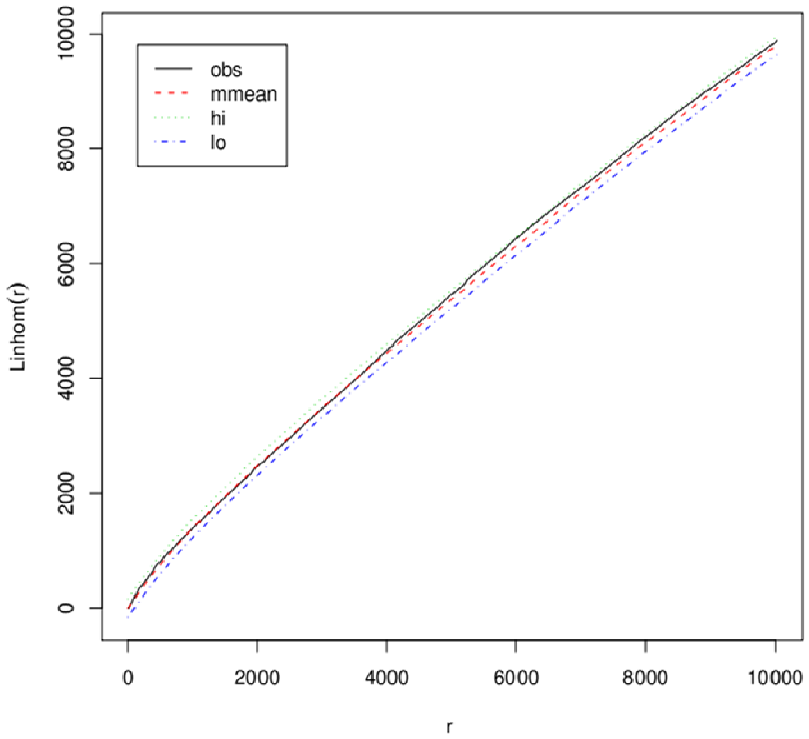

b

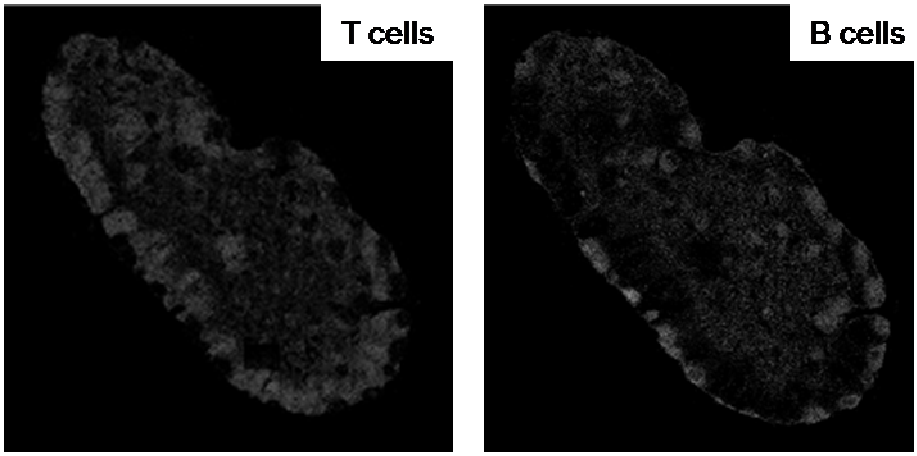

Figure C15. Representative graph and images of spatial distribution of B cells which is not similar to T cells. a), The L function of B cells, indicated by the solid line, exited the confidence envelope (indicated by the light-blue and dark-blue dotted and dash lines, respectively) of T cells. b), Images of T cell and B cell distributions on a lymph node cross section, showing tighter clumps of B cells compared to the T cells.

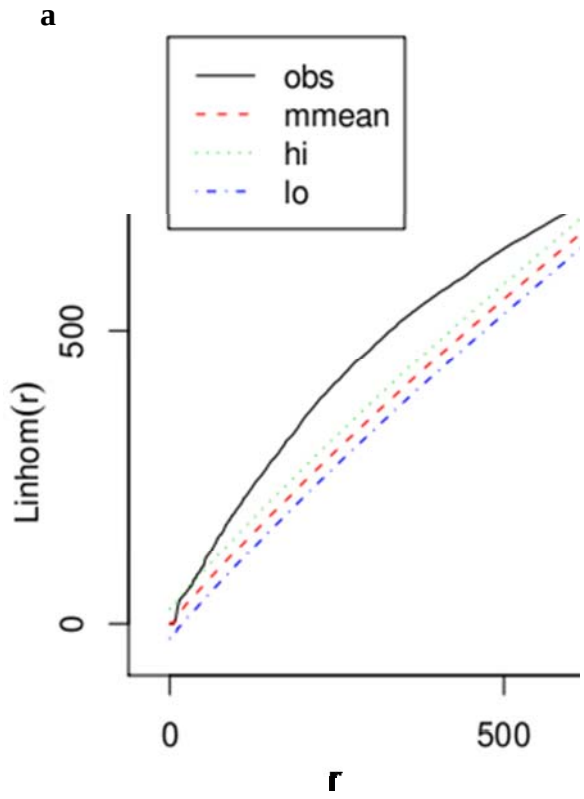

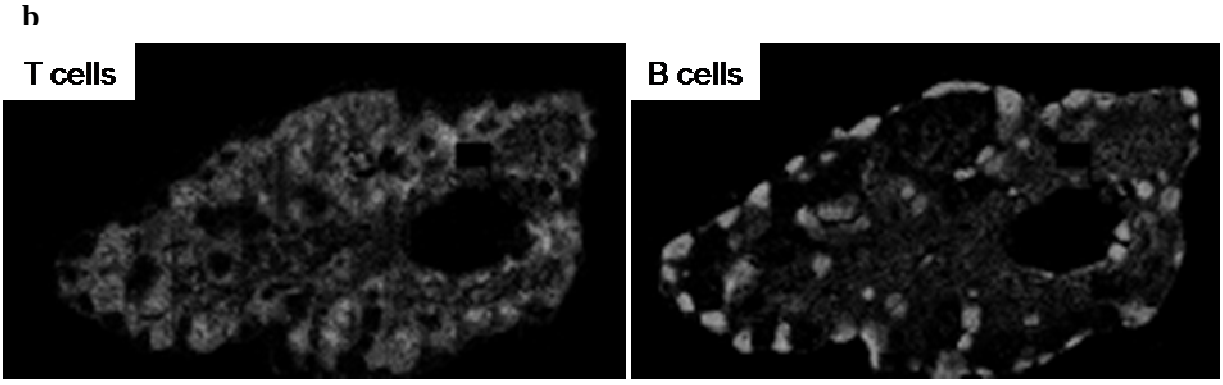

Figure C16. L function of tumor cells which fell below the envelope of the T cells, confirming tumor cells' nuclei were further apart from each other compared to T cells' nuclei within a section of a lymph node.

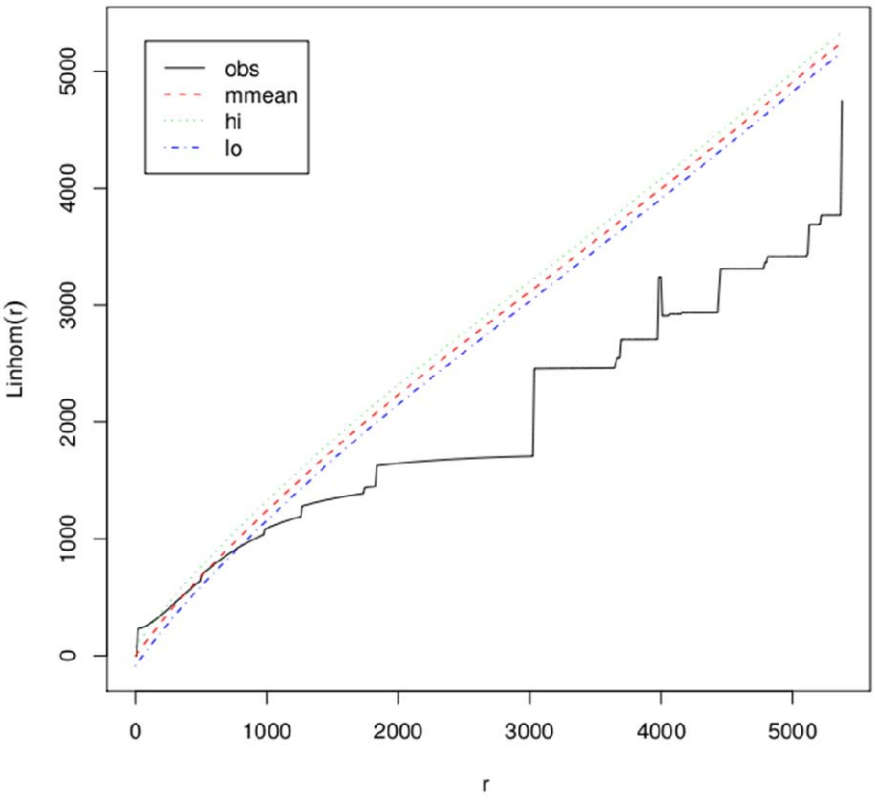

Figure C17. Simulations of time spent by the L functions of B cells outside of the T cell envelope in tumor-involved SLNs (top panel) and HLNs (bottom panel).

SLNs+ (n=15)

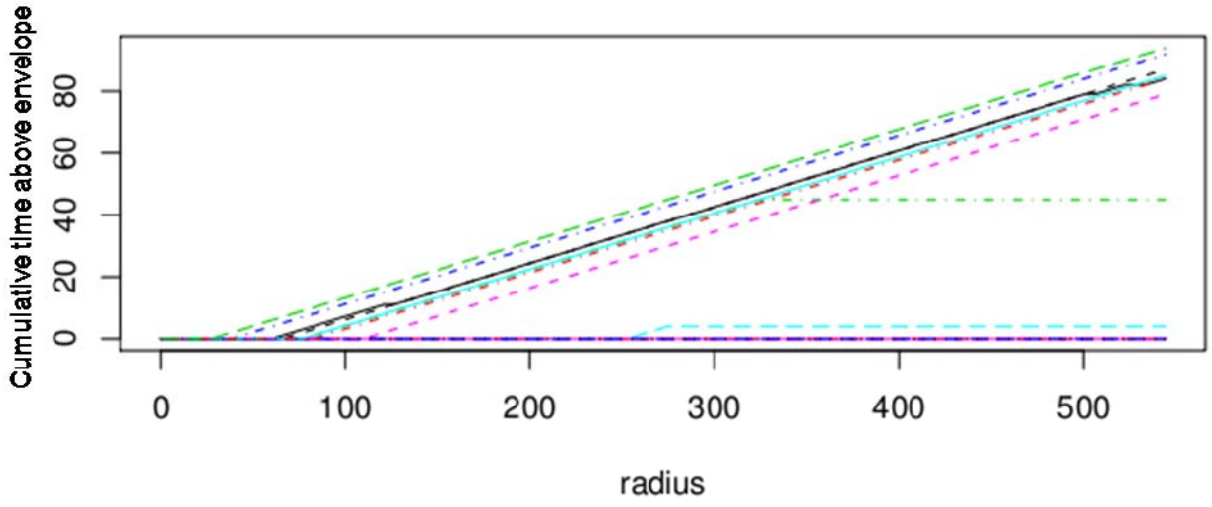

Healthy LNs (n=7)

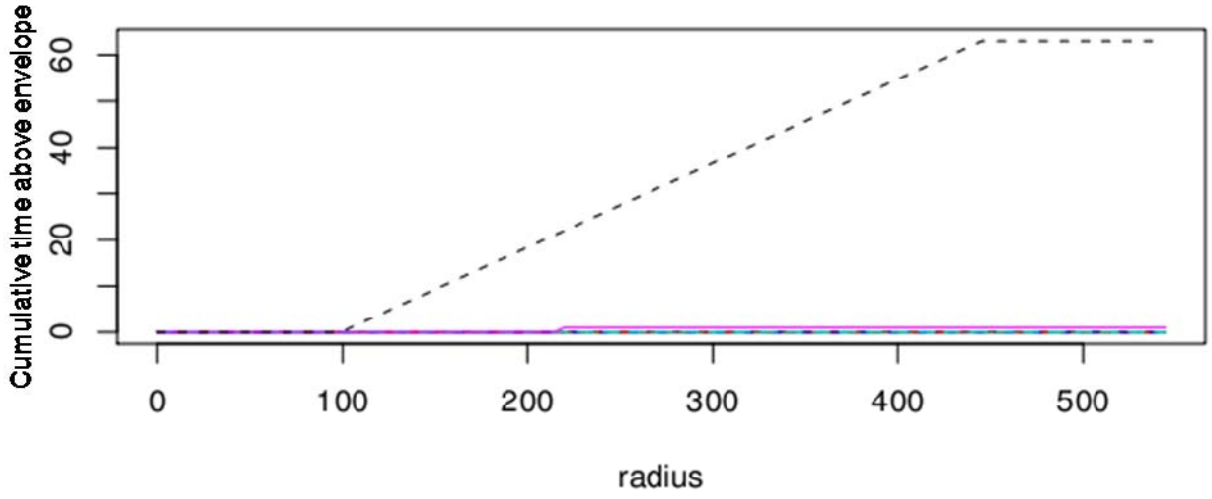

Personnel: Lee, Holmes, Schwartz, Setiadi.

D. Synthesizing a useful model of breast cancer through mathematical and computational modeling

> Originally proposed in SOW:
> To integrate our experimental data and observations into a mathematical model to address the dynamics of cancer cells and the immune response in the tumor and lymph node. This will ultimately enable us to perform *in silico* experiments to quickly test novel therapeutic strategies for breast cancer.

Due to our substantial progress and resources needed for the immunological, microarray, and histological analyses, we decided to shift resources from this mathematical modeling effort in year 4. As such, mathematical collaborators Levy and Kim did not draw any salary support from this award. We are generating substantial data that can be productively modeled in year 5 if additional resources were made available.

Overall Personnel

1. Peter P. Lee, MD – project PI (50% effort on EHSA).
2. Erich Schwartz, MD, PhD – Stanford Pathology (no salary requested on EHSA).
3. Fred Dirbas, MD – Stanford Surgical Oncology (no salary requested on EHSA).
4. Susan Holmes, PhD – Stanford Statistics (1 month per year, as 33% of 3-month summer period).
5. HongXiang Yu, PhD - post-doc 1, 75% effort on EHSA – immunological and microarray studies.
6. Ning Yan, PhD - post-doc 2, 100% effort on EHSA – data analysis.
7. Diana Simons - research assistant 1, 100% effort on EHSA – to aid in immunological, histology, and microarray studies.

KEY RESEARCH ACCOMPLISHMENTS:

- Recruited over 240 breast cancer patients to-date into this study, acquiring tumor, TDLNs, and/or blood samples for analyses.
- Demonstrated a defect in IFN signaling in peripheral blood lymphocytes from breast cancer patients.
- Discovered perturbations in BCR signaling in memory B cells from breast cancer patients.
- Completion of a second batch microarray experiment and a more in-depth analysis of the complete microarray data set.
- Identified gene expression patterns within TDLNs which show blunted proliferation of immune cells and may lead to mechanistic insights.
- Identification of a Polycomb repression signature in metastatic tumor cells isolated from TDLNs.
- Optimization of multiple 5-color IHC staining combinations
- Demonstrated altered proportions of immune cells in TDLNs

Outline of the project plan for the next 12 months

- Continue recruiting patients into study and acquiring samples.
- Continue functional assays of lymphocytes from tumor, TDLNs, and peripheral blood.
- Continue to determine the molecular basis of IFN signaling perturbations in PBMCs from breast cancer patients.
- Continue microarray analysis of patient sample sets. Each set includes tumor cells, tumor infiltrating immune cells, immune cells from TDLN, and immune cells from blood.
- Continue to assay additional breast cancer and healthy control PBMCs to interrogate TCR signaling
- Continue IHC staining for follicular dendritic cells, follicular T helper cells, histiocytes and apoptotic cells.
- If additional resources can be made available, we will integrate these data using mathematical modeling and computer simulations.

REPORTABLE OUTCOMES:

1. Critchley-Thorne RJ, Simons DL, Yan N, Miyahira AK, Dirbas FM, Johnson DL, Swetter SM, Carlson RW, Fisher GA, Koong A, Holmes S, **Lee PP**. Impaired interferon signaling is a common immune defect in human cancer. Proc Natl Acad Sci U S A. 2009 Jun 2;106(22):9010-5. PMID: 19451644

2. Setiadi AF, Kohrt HB, Schwartz E, Johnson D, Holmes SP, and **Lee PP**. Quantitative, Architectural Analysis of Tumor-Draining Lymph Nodes. Under Revision.

CONCLUSIONS:

In year 4, the foundation we have built over the first three years of this award have enabled us to make substantial progress in multiple areas of this project. We now have an efficient system in place to recruit patients into this study and procure their samples, with a total of 240 subjects recruited to-date. Limited amounts of clinical materials available from each subject remains major challenges to the success of this project – we continually attempt to address and solve this issue by reducing the cell numbers that we need for each assay. We have further enhanced and refined a powerful set of immunological assays and molecular tools to study these samples in greater detail than previously possible. We continue to uncover dramatic changes in the immune cell populations within tumors, TDLNs, and peripheral blood from breast cancer patients. These findings are reported above, and have led to a high profile publication in PNAS, but more to come in year 5. The coming final year of this award will see more progress and insights.

REFERENCES:

Baddeley, A., *et al*., Case Studies in Spatial Point Process Modeling, (Springer, Inc., New York, 2005).

Carpenter, EL., *et al*, Collapse of the CD27+ B-cell compartment associated with systemic plasmacytosis in patients with advanced melanoma and other cancers. Clin Cancer Res. 2009;15(13):4277-87.

Critchley-Thorne, R., *et al*. Down-Regulation of the Interferon Signaling Pathway in T Lymphocytes from Patients with Metastatic Melanoma. PLoS Medicine 2007; 4:0897

Critchley-Thorne, R., *et al*. Impaired Interferon Signaling is a Common Defect in Cancer. PNAS 2009; Jun 2;106 (22)

Diggle, P.J. Statistical Analysis of Spatial Point Patterns, (Academic Press, New York, 2003).

Dixon, P.M. Ripley's K function. in Encyclopedia of Environmetrics, Vol. 3 (ed. El-Shaarawi, A.H., Piegorsch, W. W.) 1796–1803 (John Wiley & Sons, Ltd, Chichester, 2002).

Kraal, G., *et al*. The importance of regional lymph nodes for mucosal tolerance. Immunol Rev. 2006;213:119-30.

APPENDICES: None at this time.

SUPPORTING DATA: Tables and figures are integrated into the text above